drugs and drug candidates

MDPI

Article

Synthesis and Antimalarial Evaluation of New 1,3,5-*tris*[(4-(Substituted-aminomethyl)phenyl)methyl]benzene Derivatives: A Novel Alternative Antiparasitic Scaffold

Sandra Albenque-Rubio [1], Jean Guillon [1,*], Anita Cohen [2], Patrice Agnamey [3], Solène Savrimoutou [1], Stéphane Moreau [1], Jean-Louis Mergny [4], Luisa Ronga [5], Ioannis Kanavos [5], Serge Moukha [6,7], Pascale Dozolme [6,7] and Pascal Sonnet [3]

1 Faculty of Pharmacy, University of Bordeaux, CNRS, INSERM, ARNA, UMR 5320, U1212, F-33000 Bordeaux, France; sandra.rubio@u-bordeaux.fr (S.A.-R.); solene.savrimoutou@u-bordeaux.fr (S.S.); stephane.moreau@u-bordeaux.fr (S.M.)
2 Faculty of Pharmacy, University of Aix-Marseille Inserm U1261, MCT-UMR MD1, F-13005 Marseille, France; anita.cohen@univ-amu.fr
3 Faculty of Pharmacy, Agents Infectieux, Résistance et Chimiothérapie (AGIR), UR 4294, UFR de Pharmacie, University of Picardie Jules Verne, F-80037 Amiens, France; p.agnamey@u-picardie.fr (P.A.); pascal.sonnet@u-picardie.fr (P.S.)
4 Laboratoire d'Optique et Biosciences, Institut Polytechnique de Paris, Ecole Polytechnique, CNRS, INSERM, F-91128 Palaiseau, France; jean-louis.mergny@inserm.fr
5 Institut des Sciences Analytiques et de Physico-Chimie Pour l'Environnement et les Matériaux, Université de Pau et des Pays de l'Adour, E2S UPPA, CNRS, IPREM, F-64053 Pau, France; luisa.ronga@univ-pau.fr (L.R.); i.kanavos@univ-pau.fr (I.K.)
6 Centre de Recherche Cardio-Thoracique de Bordeaux (CRCTB), UMR U1045 INSERM, PTIB—Hôpital Xavier Arnozan, F-33600 Pessac, France; serge.moukha@u-bordeaux.fr (S.M.); pascale.dozolme@u-bordeaux.fr (P.D.)
7 INRAE Bordeaux Aquitaine, F-33140 Villenave-d'Ornon, France
* Correspondence: jean.guillon@u-bordeaux.fr; Tel.: +33-(0)5-57-57-16-52

Abstract: A series of new 1,3,5-*tris*[(4-(substituted-aminomethyl)phenyl)methyl]benzene compounds were designed, synthesized, and evaluated *in vitro* against two parasites (*Plasmodium falciparum* and *Leishmania donovani*). The biological results showed antimalarial activity with IC_{50} values in the sub and μM range. The *in vitro* cytotoxicity of these new aza polyaromatic derivatives was also evaluated on human HepG2 cells. The 1,3,5-*tris*[(4-(substituted-aminomethyl)phenyl)methyl]benzene **1m** was found as one of the most potent and promising antimalarial candidates with a ratio of cytotoxic to antiprotozoal activities of 83.67 against the *P. falciparum* CQ-sensitive strain 3D7. In addition, derivative **1r** was also identified as the most interesting antimalarial compound with a selectivity index (SI) of 17.28 on the W2 *P. falciparum* CQ-resistant strain. It was previously described that the telomeres of *P. falciparum* could be considered as potential targets of these kinds of aza heterocycles; thus, the ability of these new derivatives to stabilize the parasitic telomeric G-quadruplexes was measured through a FRET melting assay.

Keywords: antimalarial activity; 1,3,5-*tris*[(4-(substituted-aminomethyl)phenyl)methyl]benzene; antileishmanial activity

check for updates

Citation: Albenque-Rubio, S.; Guillon, J.; Cohen, A.; Agnamey, P.; Savrimoutou, S.; Moreau, S.; Mergny, J.-L.; Ronga, L.; Kanavos, I.; Moukha, S.; et al. Synthesis and Antimalarial Evaluation of New 1,3,5-*tris*[(4-(Substituted-aminomethyl)phenyl)methyl]benzene Derivatives: A Novel Alternative Antiparasitic Scaffold. *Drugs Drug Candidates* **2023**, *2*, 653–672. https://doi.org/10.3390/ddc2030033

Academic Editor: Philippe Loiseau

Received: 6 June 2023
Revised: 17 July 2023
Accepted: 1 August 2023
Published: 8 August 2023

1. Introduction

One year ago, in June 2022, the World Health Organization (WHO) published guidance on new and updated recommendations for malaria [1], which were last updated on 14 March 2023 [2]. These guidelines encourage countries to tailor the recommendations to local disease settings for maximum impact. Indeed, even with the remarkable efforts during the COVID-19 pandemic to maintain services, malaria control efforts have recently

faced many health system challenges such as long-term humanitarian crisis and the undoubtable influence of climate change on the spread of this public health problem. In 2021, there was an estimated increase of 2 million malaria cases worldwide (247 million cases recorded in 84 malaria-endemic countries compared to 245 million in 2020 according to the last WHO malaria report) with most of this increase coming from countries in the WHO African Region [3]. Current challenges include the invasion in Africa by *Anopheles stephensi*, a mosquito able to adapt easily to urban environments, which poses a real risk to public health, in addition to the growing problems of resistance to insecticide-treated nets and to antimalarial drugs. Furthermore, these difficulties have impacted the control of all vector-borne neglected tropical diseases, such as leishmaniasis [4]. To this end, a global strategy was proposed by WHO in the program "Ending the neglect to attain the sustainable development goals: a road map for neglected tropical diseases 2021–2030" [5] developed through a global consultation worldwide according to which "research and innovation are fundamental enablers of programmatic progress for all (neglected) tropical diseases". It, thus, seems essential to integrate and increase cross-cutting approaches, such as new treatment approaches and investigation of community-based and applied research for several tropical diseases.

Thus, another original strategy to discover new treatments against malaria is to generate and synthesize quinoline-based derivatives that are not recognized by the protein system involved in drug efflux, such as primaquine (PQ) or amodiaquine (AQ). The efflux pumps could serve both as natural defense mechanisms and lead to the bioavailability and disposition of drugs. Originally, such a mechanism was suggested in *Plasmodium falciparum*, where red blood cells infected with CQ-resistant parasites accumulated specifically less drug than the sensitive ones, before its further analysis led to the identification of the Pfcrt gene among other quinoline compound resistance mechanisms. Such novel series that have not been recognized by the protein system involved in the drug efflux of bisquinoline A and bisacridine B antimalarial drugs (Figure 1, compounds A–B and Piperaquine) have been described in previous works [6–11]. These new compounds have much lower resistance indices than CQ, indicating that these bis-heterocyclic derivatives are less efficiently rejected by efflux by drug-resistant parasites.

During our research, we focused on the discovery of novel aza heterocyclic compounds that can be useful in antiprotozoal chemotherapy [12–20]; we have formerly developed various series of 2,9-*bis*[(substituted-aminomethyl)phenyl]phenanthrolines (series A-B), 2,4-*bis*[(substituted-aminomethyl)phenyl]quinolines, 1,3-*bis*[(substituted-aminomethyl)phenyl]isoquinoline and 2,4-*bis*[(substituted-aminomethyl)phenyl]quinazoline derivatives (series C) designed as antiprotozoal candidates, which could bind to *Plasmodium falciparum* DNA G-quadruplexes [17–20] in order to bypass the resistance mechanisms deployed by the parasites and also based on efflux. Indeed, it has previously been described that the telomeres of various protozoa could constitute attractive drug targets [21–24], and telomerase activity is observed in gametocytes and during the transition to the erythrocytic stage of the parasite *P. falciparum* [25]. The telomeric 3′ G-overhang area of *P. falciparum* is a repetition of degenerate unit 5′GGGTTYA3′ (where Y could be T or C) [26], which can fold into intramolecular G-quadruplex [27]. This difference between parasitic and human (5′GGGTTA3′) G-quadruplexes is also noticed with *Leishmania* spp., which opens the possibility of developing antiprotozoal ligands specifically targeting G-quadruplexes present in these parasitic species.

By considering our research competence in the domain of the preparation of new antiprotozoal heterocyclic derivatives, we describe here the design and synthesis of new 1,3,5-*tris*[(4-(substituted-aminomethyl)phenyl)methyl]benzene derivatives **1**, a novel alternative and potential antiparasitic scaffold against malaria. We hypothesized that substitution with three diaminobenzyl moieties in positions 1, 3, and 5 of the benzene ring could lead to more potent G4 ligands in terms of selectivity by enlarging the aromatic surface. We judged that the extended aromatic moieties of the diaminobenzyl groups would provide a basis for π–π stacking interactions with the different G-quartets. In addition, the length of

the polyamine side chains could have an influence on the stabilization and flexibility of our ligands.

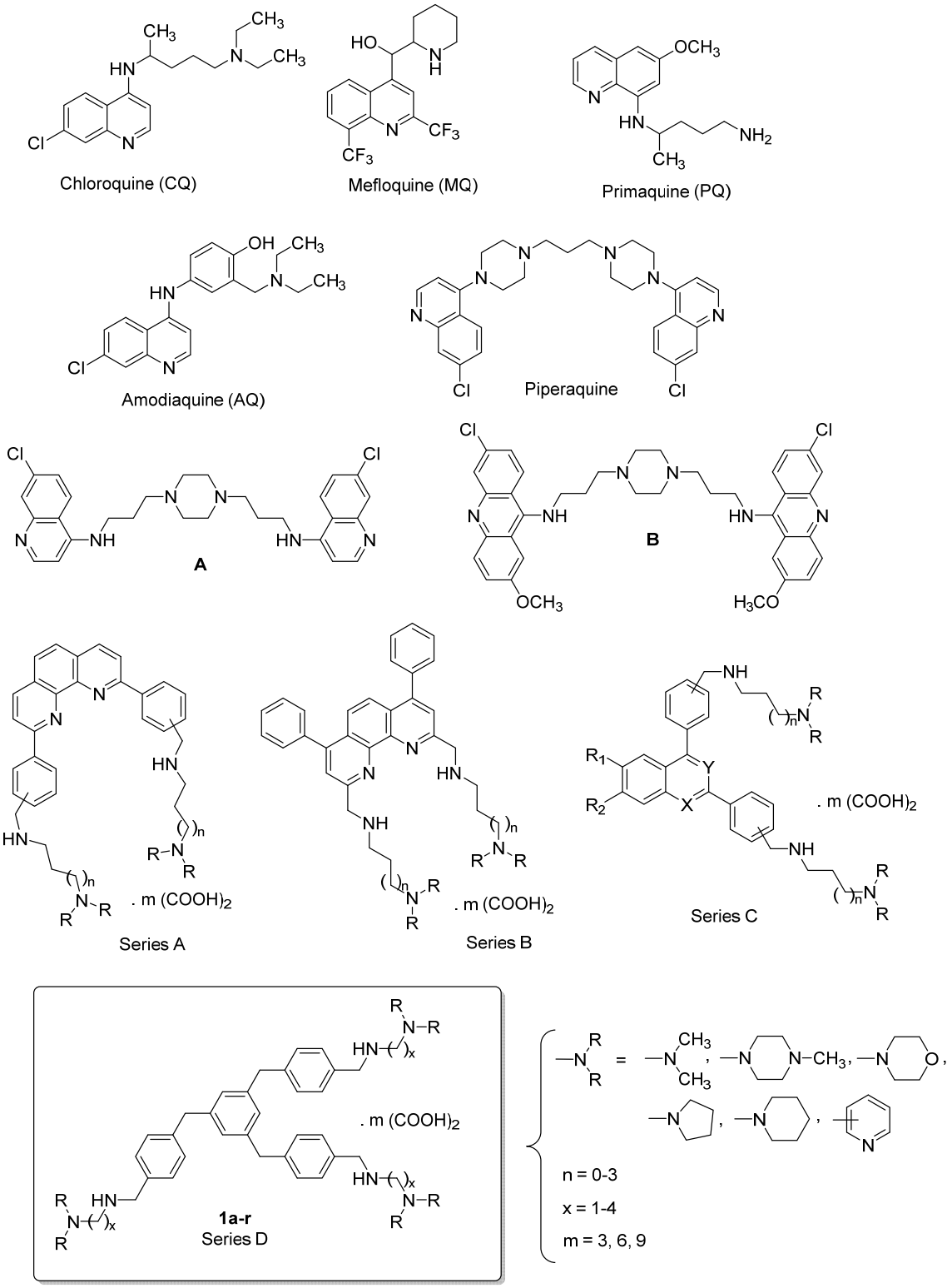

Figure 1. The structures of chloroquine (CQ), mefloquine (MQ), primaquine, amodiaquine (AQ), piperaquine, bisquinoline **A**, bisacridine **B**, phenanthrolines series A and B, quinolines/quinazoline/isoquinolines series C and newly synthesized 1,3,5-*tris*[(4-(substituted-aminomethyl)phenyl)methyl]benzene derivatives **1a-r** (Series D).

We refer to their *in vitro* antiprotozoal activities against the CQ-sensitive (3D7) and the CQ-resistant (W2) strains of the malaria parasite *P. falciparum*. These novel synthesized derivatives were also tested for *in vitro* efficacy against protozoans *Leishmania donovani*. The in vitro cytotoxicity of our 1,3,5-*tris*[(4-(substituted-aminomethyl)phenyl)methyl]benzene derivatives **1** was also assessed in human HepG2 cells, and the index of selectivity and the ratio of cytotoxic to antiprotozoal activity were determined for each compound. In addition, we investigated whether these novel polyaromatic compounds could lead to the stabilization of some parasitic telomeric DNA G-quadruplex structures. Thus, the potential stabilization of *P. falciparum* telomeric G-quadruplexes was estimated using a FRET melting assay.

2. Results

2.1. Chemistry

These newly reported 1,3,5-*tris*[(4-(substituted-aminomethyl)phenyl)methyl]benzene derivatives **1a-r** were synthesized starting from commercially available 1,3,5-*tris*(bromomethylbenzene (Scheme 1). The intermediate 1,3,5-*tris*[(4-formylphenyl)methyl]benzene **2** was prepared by a triple Suzuki–Miyaura cross-coupling reaction of 1,3,5-tris(bromomethylbenzene with an excess of 4-formylphenylboronic acid in the presence of $Pd(PPh_3)_4$ and sodium carbonate [28,29]. The reaction of various primary substituted alkylaminoalkylamines with trialdehyde **2** led to the 1,3,5-*tris*[(4-(substituted-iminomethyl)phenyl)methyl]benzenes **3a-r**, which were then reduced into the 1,3,5-*tris*[(4-(substituted-aminomethyl)phenyl)methyl]benzene derivatives **4a-r** by using sodium borohydride in methanol, as previously described by our team [17–20]. These new 1,3,5-*tris*[(4-(substituted-aminomethyl)phenyl)methyl]benzene derivatives **4a-r** were then converted into ammonium oxalate salts **1a-r** by reaction with oxalic acid in isopropanol. Table 1 gives the physical properties of these new ammonium oxalates **1a-r**.

Table 1. Physical properties of ammonium oxalate salts **1a-r**.

Compound		Salt [a]	mp (°C) [b]	% Yield [c]
1a	Beige crystals	6 $(COOH)_2$	239–241	97
1b	Grey crystals	6 $(COOH)_2$	241–242	84
1c	Beige crystals	6 $(COOH)_2$	177–179	68
1d	White crystals	9 $(COOH)_2$	209–211	73
1e	White crystals	9 $(COOH)_2$	189–191	99
1f	White crystals	6 $(COOH)_2$	175–177	57
1g	Beige crystals	6 $(COOH)_2$	167–169	61
1h	White crystals	6 $(COOH)_2$	189–191	70
1i	Yellow crystals	3 $(COOH)_2$	140–142	52
1j	Yellow crystals	3 $(COOH)_2$	151–153	88
1k	Orange crystals	3 $(COOH)_2$	159–161	98
1l	Yellow crystals	3 $(COOH)_2$	174–176	81
1m	Beige crystals	3 $(COOH)_2$	185–187	82
1n	Orange crystals	3 $(COOH)_2$	159–161	98
1o	Beige crystals	3 $(COOH)_2$	181–183	95
1p	Grey crystals	3 $(COOH)_2$	157–159	57
1q	Beige crystals	3 $(COOH)_2$	171–173	73
1r	White crystals	3 $(COOH)_2$	178–180	98

[a] The stoichiometry and composition of the salts were determined using elemental analyses, and obtained values were within ±0.4% of the theoretical values. [b] Crystallization solvent: 2-PrOH–H_2O. [c] The yields only included the conversions into the ammonium oxalates.

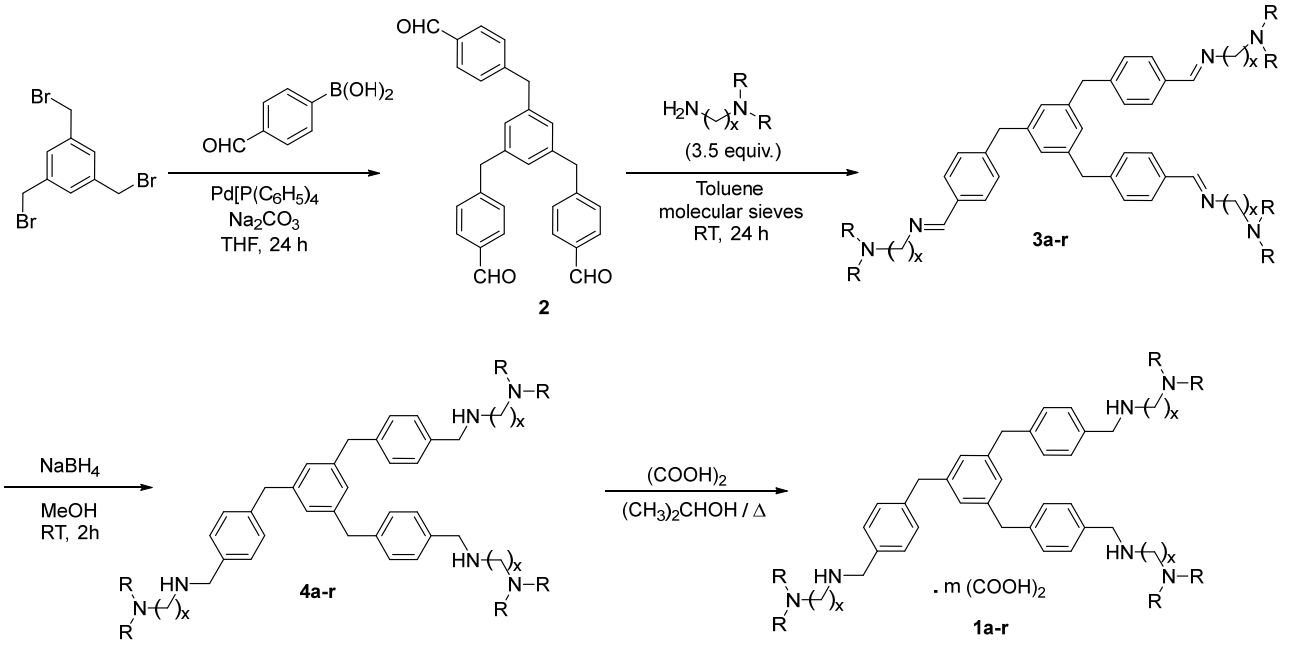

		x	m
3a, **4a**, **1a**	$-N(CH_3)_2$	2	6
3b, **4b**, **1b**	$-N(CH_3)_2$	3	6
3c, **4c**, **1c**	$-N(CH_3)_2$	4	6
3d, **4d**, **1d**	$-N$ $N-CH_3$	2	9
3e, **4e**, **1e**	$-N$ $N-CH_3$	3	9
3f, **4f**, **1f**	$-N$ O	3	6
3g, **4g**, **1g**	$-N$	3	6
3h, **4h**, **1h**	$-N$	3	6
3i, **4i**, **1i**		0	3

		x	m
3j, **4j**, **1j**		1	3
3k, **4k**, **1k**		2	3
3l, **4l**, **1l**		3	3
3m, **4m**,**1m**		1	3
3n, **4n**, **1n**		2	3
3o, **4o**, **1o**		3	3
3p, **4p**, **1p**		1	3
3q, **4q**, **1q**		2	3
3r, **4r**, **1r**		3	3

Scheme 1. General procedure for the preparation of 1,3,5-*tris*[(4-(substituted-aminomethyl)phenyl)-methyl]benzene derivatives **1a-r**.

2.2. Biological Evaluation

2.2.1. In Vitro Antimalarial Activity

Most of these novel 1,3,5-*tris*[(4-(substituted-aminomethyl)phenyl)methyl]benzene compounds **1a-r** were tested for their *in vitro* antimalarial activity by incubation with *P. falciparum* CQ-resistant strain W2 (IC_{50} CQ = 0.40 μM, IC_{50} MQ = 0.016 μM) and the strain 3D7, which is CQ-sensitive and has decreased sensitivity to MQ (IC_{50} CQ = 0.11 μM, MQ = 0.06 μM). The IC_{50} values of these new 1,3,5-*tris*[(4-(substituted-aminomethyl)phenyl)-methyl]benzenes **1** were found between 0.18 and 24.82 μM against W2 and between 0.07 and 25.78 μM against the 3D7 *P. falciparum* strains (Table 2).

Table 2. In vitro sensitivity of *P. falciparum* and *L. donovani* strains to compounds **1a-r** and cytotoxicity of these compounds in HepG2 cells.

Compound	*P. falciparum* Strains IC_{50} Values (μM) [a]		*L. donovani* IC_{50} Values (μM) [b]	Cytotoxicity to HepG2 Cells CC_{50} Values (μM) [c]
	W2	3D7		
CQ [d]	0.40 ± 0.04	0.11 ± 0.01	n.d. [g]	30
MQ [d]	0.016 ± 0.002	0.06 ± 0.003	n.d. [g]	n.d. [f]
Pentamidine [e]	n.d. [f]	n.d. [f]	5.5 ± 0.80	2.3 ± 0.50
Amphotericin B [e]	n.d. [f]	n.d. [f]	0.1 ± 0.04	8.8 ± 0.60
1a	>40	3.29 ± 0.81	>15.6 [g]	22.33 ± 0.89
1b	15.63 ± 0.32	15.01 ± 0.61	>15.6 [g]	72.90 ± 3.66
1c	>40	20.41 ± 0.42	>15.6 [g]	70.38 ± 4.41
1d	24.82 ± 0.28	11.25 ± 1.25	>15.6 [g]	51.82 ± 2.00
1e	15.46 ± 0.64	6.71 ± 1.24	>15.6 [g]	32.34 ± 2.52
1f	3.27 ± 0.42	1.18 ± 0.17	>15.6 [g]	25.35 ± 1.60
1g	13.28 ± 0.86	8.64 ± 0.79	>15.6 [g]	18.49 ± 0.52
1h	14.43 ± 2.55	7.22 ± 0.88	>15.6 [g]	18.68 ± 1.72
1i	>40	>40	>15.6 [g]	>100
1j	0.79 ± 0.28	0.71 ± 0.25	>15.6 [g]	11.70 ± 0.60
1k	1.54 ± 0.64	0.66 ± 0.23	>15.6 [g]	2.59 ± 0.14
1l	0.63 ± 0.40	0.42 ± 0.12	>15.6 [g]	2.44 ± 0.31
1m	4.82 ± 0.98	0.30 ± 0.05	>15.6 [g]	25.10 ± 2.05
1n	0.43 ± 0.10	0.26 ± 0.05	>15.6 [g]	2.78 ± 0.18
1o	0.63 ± 0.16	25.78 ± 2.06	14.04 ± 1.1	2.12 ± 0.18
1p	n.d. [f]	0.93 ± 0.21	>15.6 [g]	2.36 ± 0.52
1q	0.29 ± 0.02	>40	5.96 ± 0.50	2.00 ± 0.21
1r	0.18 ± 0.05	0.07 ± 0.03	6.44 ± 1.20	3.11 ± 0.76

[a] Values were measured against CQ-resistant and mefloquine-sensitive strain W2 and the CQ-sensitive and MQ decreased sensitivity strain 3D7. [b] IC_{50} values were measured against the promastigotes of *Leishmania donovani* strain. The IC_{50} (μM) values correspond to the means +/− standard deviations from 3 independent experiments. [c] CC_{50} values were measured against HepG2 cells. The CC_{50} (μM) values correspond to the means +/− standard deviations from 3 independent experiments. [d] CQ and MQ were used as antiplasmodial compounds of reference. [e] Pentamidine and amphotericin B were used as antileishmanial compounds of reference. [f] n.d.: not determined. [g] Molecule was not tested at higher concentrations (not active).

In this novel series, all 1,3,5-*tris*[(4-(substituted-aminomethyl)phenyl)methyl]benzenes bearing pyridinylalkylaminomethyl side chains at position 4 of the benzyl rings (compounds **1j-r**) displayed better activities than their homologs substituted with alkylaminoalkylaminomethyl side chains (compounds **1a-h**); i.e., IC_{50} = 0.18 to 4.82 μM for **1j-r** versus IC_{50} = 3.27 to >40 μM for **1a-h**. Against the *P. falciparum* CQ-resistant strain W2, 1,3,5-*tris*-[(4-(substituted-aminomethyl)phenyl)methyl]benzene **1r** bearing pyridin-4-ylpropylaminomethyl side chains at position 4 of each of the benzyl groups was noticed to be the most active, with an IC_{50} of 0.18 μM. From a general point of view, the substitution of the side chains by C_3 alkyl chains showed better antimalarial activities against the W2 strain than their C_1, C_2, or C_4 homologs: for example, IC_{50} = 0.63 μM for **1l** in comparison with 0.79 and 1.54 μM for **1j** and **1k**, respectively, or 15.63 μM for **1b** versus >40 μM for **1a** and **1c**. In addition, compound **1f**, substituted by 3 morpholinopropylaminomethyl chains, was found to be more active than its other substituted aminoalkylaminomethyl homologs **1a-e** and **1g-h** (IC_{50} = 3.27 μM for **1f** versus IC_{50} = 13.28 to >40 μM for **1a-e** and **1g-h**).

Against the 3D7 CQ-sensitive strain, the 1,3,5-*tris*[(4-(pyridin-4-ylpropylaminomethyl)-phenyl)methyl]benzene **1r** was the most potent antiplasmodial derivative with an IC_{50} of 0.07 μM. This is very similar to the IC_{50} values of the two reference drugs, CQ and MQ, which presented IC_{50} values of 0.11 and 0.06 μM, respectively. In terms of structure–activities relationships, we could also conclude the same observations as those noticed for the W2 strain, with the exception of compounds **1o** and **1q**, which were surprisingly found as the less bioactive derivatives, with an IC_{50} of 25.78 and >40 μM, respectively,

against the 3D7 *P. falciparum* strain. Similarly, compound **1f** remained the compound exhibiting the best antimalarial activity against the 3D7 strain in the subseries of the 1,3,5-*tris*[(4-(substituted-aminoalkylaminomethyl)phenyl)methyl]benzene derivatives **1a-e** and **1g-h**, i.e., IC_{50} = 1.18 μM for **1f** versus 3.29 to 20.41 μM for the other compounds.

Surprisingly, derivative **1i** bearing three quinoline nuclei, a motif found in the reference molecules CQ and MQ, did not show any antimalarial activity on the two *P. falciparum* strains tested (IC_{50} > 40 μM). Moreover, we also noticed that the majority of our novel compounds **1**, except derivatives **1o** and **1q**, were found more active against the CQ-sensitive and MQ-resistant *P. falciparum* strain 3D7 than against the CQ-resistant and mefloquine-sensitive *P. falciparum* strain W2.

2.2.2. In Vitro Antileishmanial Activity against Promastigote Forms

In order to better understand the biological profile of our novel 1,3,5-*tris*[(4-(substituted-aminomethyl)phenyl)methyl]benzene heterocycles **1a-r**, some additional antiprotozoal analyses were then performed. Thus, *in vitro* activity against the parasite *L. donovani* was biologically evaluated (Table 2). The reference drugs pentamidine and amphotericin B presented IC_{50} values of 5.50 μM and 0.10 μM, respectively, against *L. donovani*. Only 1,3,5-*tris*[(4-(substituted-aminomethyl)phenyl)methyl]benzenes **1n**, **1q**, and **1r** were found slightly bioactive against the promastigote forms of *L. donovani* with an IC_{50} of 14.04, 5.96, and 6.44 μM, respectively. In terms of structure—activity relationships, these pharmacological results demonstrate that the activity of these new compounds seems to be related to the presence of an ethyl or propyl group substituted by a pyridine in the three lateral chains. Regrettably, none of all of our other novel derivatives **1** showed any anti-leishmanial activity *in vitro* (all IC_{50} values > 15.6 μM).

2.2.3. Cytotoxicity and Selectivity Index

In order to assess their selectivity of action, the cytotoxicities of our novel synthesized antiparasitic 1,3,5-*tris*[(4-(substituted-aminomethyl)phenyl)methyl]benzene compounds **1a-r** were evaluated *in vitro* on the human cell line HepG2, which is a commonly used human-derived hepatocarcinoma cell line and expresses many hepatocyte-specific metabolic enzymes. The aim of this assay was the evaluation of the impact of metabolic activation of the tested derivatives on cell viability [30,31]. Thus, the cytotoxic concentrations 50% (CC_{50}) were obtained, and selectivity indices (SIs), defined as the ratios of cytotoxic to antiparasitic activities ($SI = CC_{50}/IC_{50}$), were then calculated (Table 3). Most of these novel 1,3,5-*tris*[(4-(substituted-aminomethyl)phenyl)methyl]benzene compounds **1a-r,** which were noticed less or more active against the various parasites, showed cytotoxicity against these HepG2 cells with CC_{50} values ranging from 2.00 to 72.90 μM. Against the human cell line HepG2, the 1,3,5-*tris*[(4-(substituted-aminomethyl)phenyl)methyl]benzene derivatives bearing pyridinylalkylaminomethyl side chains at position 4 of the benzyl groups (compounds **1k-r**) were found more cytotoxic, except compounds **1j** and **1m**, than their homologs substituted with alkylaminoalkylaminomethyl side chains (compounds **1a-h**), i.e., CC_{50} = 2.00 to 3.11 μM for **1k-r** versus CC_{50} = 18.49 to 72.90 μM for **1a-h**. In addition, derivative **1i**, substituted by quinoline nuclei on its three side chains, showed a cytotoxicity concentration of 50% (CC_{50}) superior to 100 μM.

Table 3. Selectivity indices of compounds **1a-r**.

Compound	Selectivity Index [a]		
	HepG2/W2	**HepG2/3D7**	**HepG2/*L. donovani***
CQ	75	272	n.d. [b]
Pentamidine	n.d. [b]	n.d. [b]	n.d. [b]
Amphotericin B	n.d. [b]	n.d. [b]	88.0
1a	0.56>	6.79	n.d. [b]
1b	4.66	4.86	n.d. [b]
1c	1.76>	3.45	n.d. [b]
1d	2.09	4.61	n.d. [b]
1e	2.09	4.82	n.d. [b]
1f	7.75	21.48	n.d. [b]
1g	1.39	2.14	n.d. [b]
1h	1.29	2.59	n.d. [b]
1i	n.d. [b]	n.d. [b]	n.d. [b]
1j	14.81	16.48	n.d. [b]
1k	1.68	3.92	n.d. [b]
1l	3.87	5.81	n.d. [b]
1m	5.21	83.67	n.d. [b]
1n	6.46	10.69	n.d. [b]
1o	3.36	0.08	0.15
1p	n.d. [b]	2.54	n.d. [b]
1q	6.90	0.05>	0.34
1r	17.28	44.43	0.48

[a] SI was defined as the ratio between the CC_{50} value on the HepG2 cells and the IC_{50} value against the *P. falciparum* W2 or 3D7 strains. [b] n.d.: not determined.

Concerning the *P. falciparum* strain W2, the calculated SIs were found between 0.56 and 17.28. For the CQ-sensitive strain 3D7, these SIs were noticed from 2.14 to 83.67. An examination of these SI data led us to identify the 1,3,5-*tris*[(4-(substituted-aminomethyl)phenyl)methyl]benzene **1r** as an interesting compound with an SI of 17.28 for the W2 strain. In addition, compound **1j** also showed an interesting SI value of 14.81 for this CQ-resistant strain W2. Moreover, the SI data also led us to the identification of the promising derivative **1m** with an SI of 83.67 for the CQ-sensitive strain 3D7. Against this 3D7 *P. falciparum* strain, 1,3,5-*tris*[(4-(substituted-aminomethyl)phenyl)methyl]benzene **1r** had an SI of 44.43 (Figure 2). These promising and interesting SI values may indicate that these new original polyaromatic benzene **1** compounds warrant further investigations into their potential use as antimalarial drugs.

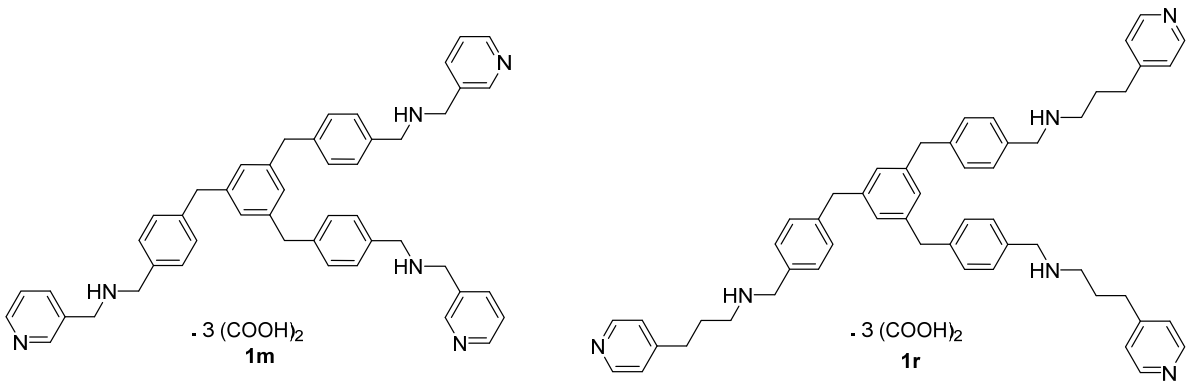

Figure 2. The structures of the most promising synthesized 1,3,5-*tris*[(4-(substituted-aminomethyl)phenyl)methyl]benzene derivatives **1m** and **1r**.

2.3. FRET Melting Experiments

As the telomeres of *P. falciparum* could be estimated as potential and interesting targets of these kinds of polyaromatic derivatives [20,25–27], we also investigated the potential stabilization of the *P. falciparum* telomeric chromosomic G-quadruplexes via some biologically active compounds **1** using a FRET melting assays. Thus, a FRET melting assay was used to determine the degree to which the novel polyaromatic compounds **1** stabilize the G-quadruplexes, which were formed by oligonucleotides with *P. falciparum* as well as human telomeric sequences. Thus, we used two fluorescently labeled *P. falciparum* telomeric chromosomic sequences (FPf1T and FPf8T) and one human telomeric sequence (F21T).

To probe the G4 selectivity of our new 1,3,5-*tris*[(4-(substituted-aminomethyl)phenyl)methyl]benzene ligands **1** over duplex DNA, a FRET melting assay was realized using a duplex control sequence, FdxT. Comparatively, we also evaluated the reference G4 ligand, named PhenDC3, and the antimalarial reference drugs, CQ and MQ. To allow a comparison of selectivities, we calculated the difference (ΔTm) between the Tm of the G-quadruplex formed by FPf1T, FPf8T, F21T, or FdxT in the presence or absence of each selected derivative. These ΔTm values are summarized in Table 4. For the selected ligands **1**, the ΔTm values ranged from 0.5 to 24.3 °C at a 2 μM derivative concentration.

Table 4. FRET melting values for selected compounds **1** (2 μM) with FPf1T, FPf8T, F21T, and FdxT (0.2 μM) in K^+ conditions.

Compound	ΔT_m (°C) [a] FPf1T		ΔT_m (°C) [a] FPf8T		ΔT_m (°C) [a] F21T		ΔT_m (°C) [a] FdxT	
PhenDC3	24.6	±0.1	24.7	±0.2	26.3	±0.1	0.1	±0.2
CQ	1.9	±0.1	2.4	±1.2	2.4	±1.1	n.d. [b]	
MQ	3.1	±0.5	6.6	±2.3	2.6	±0.5	n.d. [b]	
1b	19.6	±0.3	21.6	±0.7	18.2	±0.6	1.8	±0.2
1d	23.1	±0.4	24.3	±1.5	22.4	±3.3	3.1	±0.3
1f	6.4	±1.4	8.5	±0.8	7.3	±0.5	0.0	±0.1
1l	7.9	±0.6	10.1	±1.2	8.9	±0.5	−0.1	±0.1
1m	1.4	±0.3	1.4	±0.3	0.5	±0.4	0.1	±0.1
1n	3.6	±0.6	5.5	±1.0	3.5	±1.0	0.2	±0.0
1r	7.0	±2.0	8.7	±1.8	6.6	±0.6	−0.1	±0.1

[a] ΔT_m of FPf1T, FPf8T, F21T, and FdxT (0.2 μM) were recorded in 10 mM lithium cacodylate (pH 7.2), 10 mM KCl, 90mM LiCl. PhenDC3 was tested at 0.5 μM, whereas CQ and MQ were tested at 1 μM. Error margins correspond to SD of three replicates. [b] n.d.: not determined.

The best ligands that stabilized all three G-quadruplexes sequences (two parasitic FPf1T and FPf8T, and the human F21T) were compounds **1b** and **1d** (Table 4), with ΔTm values ranging from 18.2 to 24.3 °C. It could be observed that polyaromatic compounds substituted by three pyridinylalkylaminomethyl chains (compounds **1m**, **1n**, and **1r**) or bearing three morpholinoalkylaminomethyl chains (derivatives **1f**) exhibited a very low stabilization profile in comparison with their 3-(dimethylaminopropyl)aminomethyl or 2-(4-methylpiperazin-1-yl)ethyl)aminomethyl substituted homologs **1b** and **1d**.

A radar plot presented in Figure 3 shows that the selected compounds **1** may be able to stabilize more or less some of the G4 forming sequences.

All our novel selected polyaromatic ligands **1** were found to exhibit lower stabilization than the reference PhenDC3 ligand. No binding to duplex DNA sequence was detected by using FRET assays.

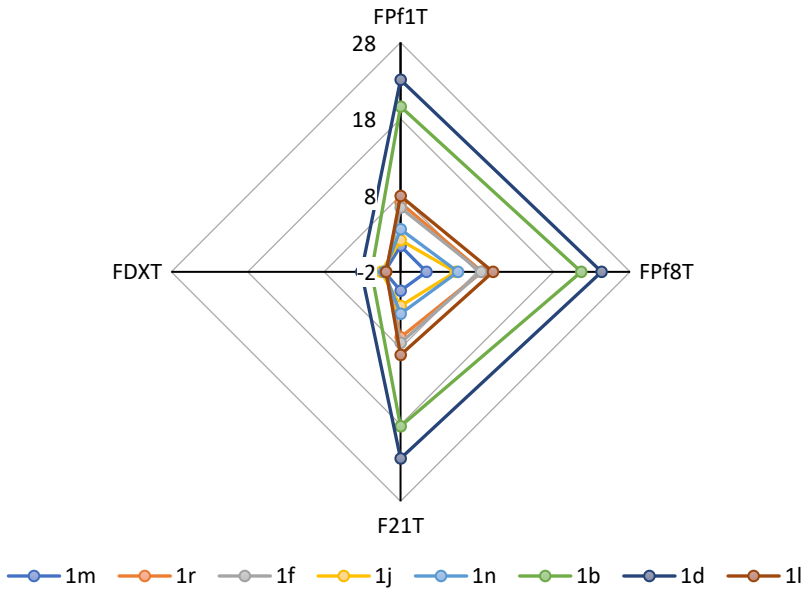

Figure 3. Stabilization specificity profile of **1b**, **1d**, **1f**, **1j**, **1l**, **1m**, **1n**, and **1r** (2 μM) toward various G4 oligonucleotides. The difference in Tm in presence and absence of **1b**, **1d**, **1f**, **1j**, **1l**, **1m**, **1n**, and **1r**, ΔTm, in °C is plotted for each sequence. Four quadruplexes and one duplex (FdxT) were tested.

3. Materials and Methods

3.1. Chemistry

3.1.1. General

Commercially available reagents were used as received without additional purification. Melting points were determined with an SM-LUX-POL Leitz hot-stage microscope and were uncorrected. NMR spectra were recorded with tetramethylsilane as an internal standard using a BRUKER AVANCE 300 spectrometer. Splitting patterns were reported as follows: s—singlet; bs—broad singlet; d—doublet; t—triplet; q—quartet; dd—double doublet; ddd—double double doublet; qt—quintuplet; m—multiplet. Analytical TLCs were carried out on 0.25 precoated silica gel plates (POLYGRAM SIL G/UV254) and visualization of compounds occurred after UV light irradiation. Silica gel 60 (70–230 mesh) was used for column chromatography. Mass spectra were recorded on an ESI LTQ Orbitrap Velos mass spectrometer (ThermoFisher, Bremen, Germany). Ionization was performed using an Electrospray ion source operating in positive ion mode with a capillary voltage of 3.80 kV and capillary temperature of 250 °C. The scan type analyzed was full scan, all MS recordings were in the m/z range between 150 and 2000 m/z. No type of fragmentation was carried out, and the resolution used for the analysis was 60.000.

3.1.2. Synthesis of the 1,3,5-*tris*[(4-formylphenyl)methyl]benzene **2**

To a suspension of 1,3,5-*tris*(bromomethyl)benzene (1.5 mmol), 4-formylphenylboronic acid (6 mmol), and $Pd(PPh_3)_4$ (0.225 mmol) in THF (40 mL) under nitrogen were added 4 mL of a 2 M aqueous solution of Na_2CO_3. The reaction mixture was refluxed for 24 h. The suspension was then evaporated to dryness and extracted with AcOEt (2 × 30 mL). The organic layer was filtered and washed with water (2 × 40 mL). The organic layer was dried over sodium sulfate, filtered, and evaporated under reduced pressure. The crude residue was purified by column chromatography on silica gel using AcOEt/Petroleum ether (*v*/*v*: 30/70) as eluent to give the pure product **2**. White crystals (57%); Mp = 222 °C. ^{1}H NMR ($CDCl_3$) δ ppm: 9.86 (s, 3H, CHO), 7.69 (d, 6H, J = 8.10 Hz, H-3$_{phen}$ and H-5$_{phen}$), 7.22 (d, 1H, J = 8.10 Hz, H-2$_{phen}$ and H-6$_{phen}$), 6.80 (s, 3H, H$_{benz}$), 3.89 (s, 1H, CH_2); ^{13}C NMR ($CDCl_3$) δ ppm: 191.1 (CO), 142.3 (C-1$_{phen}$), 142.6 (Cq-$_{benz}$), 134.4 (C-4$_{phen}$), 130.4 (C-3$_{phen}$ and C-5$_{phen}$), 128.8 (C-2$_{phen}$ and C-6$_{phen}$), 126.8 (CH$_{benz}$), 46.4 (CH_2); MALDI-TOF MS m/z $[M+H]^+$ Calcd for $C_{42}H_{41}N_6$: 432.17, Found: 433.17.

3.1.3. General Procedure for the Synthesis of 1,3,5-*tris*[(4-(substituted-iminomethyl)phenyl)methyl]benzenes **3a-r**

The 1,3,5-*tris*[(4-formylphenyl)methyl]benzene **2** (100 mg, 0.2 mmol) was dissolved in 6 mL of toluene. Activated molecular sieves 4 Å (800 mg) were introduced followed by dialkylamine (0.7 mmol). The reaction mixture was stirred in a stoppered flask for 24 h. The suspension that was obtained was filtered, washed with dichloromethane, and the solvent was removed under reduced pressure to afford the tri-imine **3**. The crude products were then used without further purification.

1,3,5-*Tris*[(4-(2-dimethylaminoethyl)iminomethyl)phenyl)methyl]benzene (**3a**)

Yellow oil (99%); ^{1}H NMR ($CDCl_3$) δ ppm: 8.36 (s, 3H, CH=N), 7.61 (d, 6H, J = 8.10 Hz, H-3$_{phen}$ and H-5$_{phen}$), 7.24 (d, 6H, J = 8.10 Hz, H-2$_{phen}$ and H-6$_{phen}$), 6.84 (s, 3H, H$_{benz}$), 3.90 (s, 6H, CH_2), 3.61 (t, 6H, J = 6.90 Hz, NCH_2), 2.15 (t, 6H, J = 6.90 Hz, NCH_2), 2.10 (s, 18H, $N(CH_3)_2$).

1,3,5-*Tris*[(4-(3-dimethylaminopropyl)iminomethyl)phenyl)methyl]benzene (**3b**)

Yellow oil (98%); ^{1}H NMR ($CDCl_3$) δ ppm: 8.36 (s, 3H, CH=N), 7.61 (d, 6H, J = 8.10 Hz, H-3$_{phen}$ and H-5$_{phen}$), 7.2 (d, 6H, J = 8.10 Hz, H-2$_{phen}$ and H-6$_{phen}$), 6.84 (s, 3H, H$_{benz}$), 3.90 (s, 6H, CH_2), 3.61 (t, 6H, J = 6.90 Hz, NCH_2), 2.15 (t, 6H, J = 6.90 Hz, NCH_2), 2.10 (s, 18H, $N(CH_3)_2$), 1.81 (qt, 6H, J = 8.40 Hz, CH_2).

1,3,5-*Tris*[(4-(4-dimethylaminobutyl)iminomethyl)phenyl)methyl]benzene (**3c**)

Yellow oil (98%); ^{1}H NMR ($CDCl_3$) δ ppm: 8.24 (s, 3H, CH=N), 7.61 (d, 6H, J = 8.1 Hz, H-3$_{phen}$ and H-5$_{phen}$), 7.17 (d, 6H, J = 8.10 Hz, H-2$_{phen}$ and H-6$_{phen}$), 6.84 (s, 3H, H$_{benz}$), 3.90 (s, 6H, CH_2), 3.61 (t, 6H, J = 6.90 Hz, NCH_2), 2.15 (t, 6H, J = 6.90 Hz, NCH_2), 2.10 (s, 18H, $N(CH_3)_2$), 1.72–1.69 (m, 6H, CH_2), 1.55–1.51 (m, 6H, CH_2).

1,3,5-*Tris*[(4-(2-(4-methylpiperazin-1-yl)ethyl)iminomethyl)phenyl)methyl]benzene (**3d**)

Yellow oil (98%); ^{1}H NMR ($CDCl_3$) δ ppm: 8.17 (s, 3H, CH=N), 7.51 (d, 6H, J = 8.10 Hz, H-3$_{phen}$ and H-5$_{phen}$), 7.17 (d, 6H, J = 8.10 Hz, H-2$_{phen}$ and H-6$_{phen}$), 6.76 (s, 3H, H$_{benz}$), 3.81 (s, 6H, CH_2), 3.66 (t, 6H, J = 6.0 Hz, NCH_2), 2.68 (t, 6H, J = 8.40 Hz, NCH_2), 2.23 (s, 24H, NCH_{2pip}), 2.18 (s, 9H, NCH_3).

1,3,5-*Tris*[(4-(3-(4-methylpiperazin-1-yl)propyl)iminomethyl)phenyl)methyl]benzene (**3e**)

Yellow oil (98%); ^{1}H NMR ($CDCl_3$) δ ppm: 8.25 (s, 3H, CH=N), 7.62 (d, 6H, J = 8.10 Hz, H-3$_{phen}$ and H-5$_{phen}$), 7.17 (d, 6H, J = 8.10 Hz, H-2$_{phen}$ and H-6$_{phen}$), 6.84 (s, 3H, H$_{benz}$), 3.90 (s, 6H, CH_2), 3.63 (t, 6H, J = 6.00 Hz, NCH_2), 2.68 (t, 6H, J = 6.00 Hz, NCH_2), 2.23 (s, 24H, NCH_{2pip}), 2.18 (s, 9H, NCH_3), 1.90–1.88 (m, 6H, CH_2).

1,3,5-*Tris*[(4-(3-(morpholin-1-yl)propyl)iminomethyl)phenyl)methyl]benzene (**3f**)

Yellow oil (94%); ^{1}H NMR ($CDCl_3$) δ ppm: 8.18 (s, 3H, CH=N), 7.56 (d, 6H, J = 8.10 Hz, H-3$_{phen}$ and H-5$_{phen}$), 7.12 (d, 6H, J = 8.10 Hz, H-2$_{phen}$ and H-6$_{phen}$), 6.79 (s, 3H, H$_{benz}$), 3.84 (s, 6H, CH_2), 3.65 (t, 12H, J = 4.20 Hz, OCH_2), 3.58 (t, 6H, J = 6.9 Hz, NCH_2), 2.39–2.28 (m, 18H, NCH_2 and NCH_{2morph}), 1.83 (qt, 6H, J = 6.90 Hz, CH_2).

1,3,5-*Tris*[(4-(3-(pyrrolidin-1-yl)propyl)iminomethyl)phenyl)methyl]benzene (**3g**)

Yellow oil (98%); ^{1}H NMR ($CDCl_3$) δ ppm: 8.23 (s, 3H, CH=N), 7.62 (d, 6H, J = 8.1 Hz, H-3$_{phen}$ and H-5$_{phen}$), 7.14 (d, 6H, J = 8.10 Hz, H-2$_{phen}$ and H-6$_{phen}$), 6.83 (s, 3H, H$_{benz}$), 3.88 (s, 6H, CH_2), 3.63 (t, 6H, J = 6.60 Hz, NCH_2), 3.64 (t, 6H, J = 6.60 Hz, NCH_2), 2.54–2.47 (m, 18H, NCH_2 and $NCH_{2pyrrol}$), 1.79–1.74 (m, 12H, $CH_{2pyrrol}$).

1,3,5-*Tris*[(4-(3-(piperidin-1-yl)propyl)iminomethyl)phenyl)methyl]benzene (**3h**)

Yellow oil (99%); ^{1}H NMR ($CDCl_3$) δ ppm: 8.24 (s, 3H, CH=N), 7.62 (d, 6H, J = 8.10 Hz, H-3$_{phen}$ and H-5$_{phen}$), 7.18 (d, 6H, J = 8.10 Hz, H-2$_{phen}$ and H-6$_{phen}$), 6.85 (s, 3H, H$_{benz}$), 3.90 (s, 6H, CH_2), 3.63 (t, 6H, J = 6.90 Hz, NCH_2), 2.42–2.31 (m, 18H, NCH_2 and NCH_{2pip}), 1.62–1.54 (m, 18H, CH_2 and CH_{2pip}), 1.45–1.42 (m, 6H, CH_{2pip}).

1,3,5-*Tris*{[4-((quinolin-3-yl)iminomethyl)phenyl]methyl}benzene (**3i**)

Pale-yellow oil (98%); ^{1}H NMR ($CDCl_3$) δ ppm: 8.57 (s, 3H, CH=N), 8.53 (d, 3H, J = 2.70 Hz, H-2$_{quinol}$), 8.24–8.19 (m, 3H, H-8$_{quinol}$), 8.02–7.99 (m, 3H, H-5$_{quinol}$), 7.97 (d, 3H, J = 2.70 Hz, H-4$_{quinol}$), 7.61 (d, 6H, J = 7.80 Hz, H-3$_{phen}$ and H-5$_{phen}$), 7.50–7.39 (m, 6H, H-6$_{quinol}$ and H-7$_{quinol}$), 7.23 (d, 6H, J = 7.80 Hz, H-2$_{phen}$ and H-6$_{phen}$), 7.02 (s, 3H, H$_{benz}$), 3.95 (s, 6H, CH_2).

1,3,5-*Tris*[(4-(pyridin-2-ylmethyliminomethyl)phenyl)methyl]benzene (**3j**)

Pale-yellow oil (93%); ^{1}H NMR ($CDCl_3$) δ ppm: 8.53 (d, 3H, J = 6.90 Hz, H-6_{pyrid}), 8.41 (s, 3H, CH=N), 7.71–7.57 (m, 9H, H-3_{phen}, H-5_{phen} and H-4_{pyrid}), 7.29–7.10 (m, 12H, H-2_{phen}, H-6_{phen}, H-3_{pyrid} and H-5_{pyrid}), 6.84 (s, 3H, H_{benz}), 4.92 (s, 6H, NCH_2), 3.89 (s, 6H, CH_2).

1,3,5-*Tris*[(4-(pyridin-2-ylethyliminomethyl)phenyl)methyl]benzene (**3k**)

Yellow oil (97%); ^{1}H NMR ($CDCl_3$) δ ppm: 8.52 (d, 3H, J = 5.90 Hz, H-6_{pyrid}), 8.16 (s, 3H, CH=N), 7.59–7.49 (m, 9H, H-3_{phen}, H-5_{phen} and H-4_{pyrid}), 7.18–7.05 (m, 12H, J = 8.10 Hz, H-2_{phen}, H-6_{phen}, H-3_{pyrid} and H-5_{pyrid}), 6.82 (s, 3H, H_{benz}), 3.99 (t, 6H, J = 7.20 Hz, NCH_2), 3.87 (s, 6H, CH_2), 3.17 (t, 6H, J = 7.20 Hz, CH_2Pyrid).

1,3,5-*Tris*[(4-(pyridin-2-ylpropyliminomethyl)phenyl)methyl]benzene (**3l**)

Yellow oil (97%); ^{1}H NMR ($CDCl_3$) δ ppm: 8.48 (d, 3H, J = 5.80 Hz, H-6_{pyrid}), 8.20 (s, 3H, CH=N), 7.63–7.49 (m, 9H, H-3_{phen}, H-5_{phen} and H-4_{pyrid}), 7.17–7.03 (m, 12H, J = 8.10 Hz, H-2_{phen}, H-6_{phen}, H-3_{pyrid} and H-5_{pyrid}), 6.82 (s, 3H, H_{benz}), 3.87 (s, 6H, CH_2), 3.62 (t, 6H, J = 6.60 Hz, NCH_2), 2.82 (t, 6H, J = 6.60 Hz, CH_2Pyrid), 2.12 (qt, 6H, J = 6.60 Hz, CH_2).

1,3,5-*Tris*[(4-(pyridin-3-ylmethyliminomethyl)phenyl)methyl]benzene (**3m**)

Pale-yellow oil (98%); ^{1}H NMR ($CDCl_3$) δ ppm: 8.58–8.46 (m, 6H, H-2_{pyrid} and H-6_{pyrid}), 8.35 (s, 3H, CH=N), 7.67–7.62 (m, 9H, H-3_{phen}, H-5_{phen} and H-4_{pyrid}), 7.24–7.16 (m, 9H, H-2_{phen}, H-6_{phen} and H-5_{pyrid}), 6.83 (s, 3H, H_{benz}), 4.75 (s, 6H, NCH_2), 3.88 (s, 6H, CH_2).

1,3,5-*Tris*[(4-(pyridin-3-ylethyliminomethyl)phenyl)methyl]benzene (**3n**)

Yellow oil (97%); ^{1}H NMR ($CDCl_3$) δ ppm: 8.40–8.31 (m, 6H, H-2_{pyrid} and H-6_{pyrid}), 8.02 (s, 3H, CH=N), 7.52 (d, 6H, J = 7.80 Hz, H-3_{phen} and H-5_{phen}), 7.43–7.7.38 (m, 3H, H-4_{pyrid}), 7.12–7.06 (m, 9H, H-2_{phen}, H-6_{phen} and H-5_{pyrid}), 6.77 (s, 3H, H_{benz}), 3.81 (s, 6H, CH_2), 3.71 (t, 6H, J = 7.20 Hz, NCH_2), 2.83 (t, 6H, J = 7.20 Hz, CH_2Pyrid).

1,3,5-*Tris*[(4-(pyridin-3-ylpropyliminomethyl)phenyl)methyl]benzene (**3o**)

Yellow oil (97%); ^{1}H NMR ($CDCl_3$) δ ppm: 8.45 (d, 3H, J = 2.20 Hz, H-2_{pyrid}), 8.43 (dd, 3H, J = 4.80 and 1.60 Hz, H-6_{pyrid}), 8.23 (s, 3H, CH=N), 7.63 (d, 6H, J = 8.10 Hz, H-3_{phen}, and H-5_{phen}), 7.52–7.48 (m, 3H, H-4_{pyrid}), 7.22–7.18 (m, 3H, H-5_{pyrid}), 7.18 (d, 6H, J = 8.10 Hz, H-2_{phen} and H-6_{phen}), 6.85 (s, 3H, H_{benz}), 3.90 (s, 6H, CH_2), 3.61 (t, 6H, J = 6.60 Hz, NCH_2), 2.73 (t, 6H, J = 6.60 Hz, CH_2Pyrid), 2.04 (qt, 6H, J = 6.60 Hz, CH_2).

1,3,5-*Tris*[(4-(pyridin-4-ylmethyliminomethyl)phenyl)methyl]benzene (**3p**)

Pale-yellow oil (98%); ^{1}H NMR ($CDCl_3$) δ ppm: 8.51 (d, 6H, J = 5.40 Hz, H-2_{pyrid} and H-6_{pyrid}), 8.34 (s, 3H, CH=N), 7.68 (d, 6H, J = 8.10 Hz, H-3_{phen} and H-5_{phen}), 7.25–7.17 (m, 12H, H-2_{phen}, H-6_{phen}, H-3_{pyrid} and H-5_{pyrid}), 6.85 (s, 3H, H_{benz}), 4.74 (s, 6H, NCH_2), 3.85 (s, 6H, CH_2).

1,3,5-*Tris*[(4-(pyridin-4-ylethyliminomethyl)phenyl)methyl]benzene (**3q**)

Yellow oil (97%); ^{1}H NMR ($CDCl_3$) δ ppm: 8.44–8.42 (m, 6H, H-2_{pyrid} and H-6_{pyrid}), 8.06 (s, 3H, CH=N), 7.53 (d, 6H, J = 8.20 Hz, H-3_{phen} and H-5_{phen}), 7.11 (d, 6H, J = 8.20 Hz, H-2_{phen} and H-6_{phen}), 7.09–7.04 (m, 6H, H-3_{pyrid} and H-5_{pyrid}), 6.80 (s, 3H, H_{benz}), 3.84 (s, 6H, CH_2), 3.78 (t, 6H, J = 7.20 Hz, NCH_2), 2.66 (t, 6H, J = 7.20 Hz, CH_2Pyrid).

1,3,5-*Tris*[(4-(pyridin-4-ylpropyliminomethyl)phenyl)methyl]benzene (**3r**)

Yellow oil (98%); ^{1}H NMR ($CDCl_3$) δ ppm: 8.70 (d, 6H, J = 5.40 Hz, H-2_{pyrid} and H-6_{pyrid}), 8.35 (s, 3H, CH=N), 7.89 (d, 6H, J = 7.80 Hz, H-3_{phen} and H-5_{phen}), 7.48–7.35 (m, 12H, H-2_{phen}, H-6_{phen}, H-3_{pyrid} and H-5_{pyrid}), 7.11 (s, 3H, H_{benz}), 4.10 (s, 6H, CH_2), 3.78 (t, 6H, J = 7.20 Hz, NCH_2), 2.85 (t, 6H, J = 7.20 Hz, CH_2Pyrid), 2.21 (qt, 6H, J = 7.20 Hz, CH_2).

3.1.4. General Procedure for the Synthesis of 1,3,5-*tris*[(4-(substituted-aminomethyl)phenyl)methyl]benzenes **4a-r**

To a solution of compound **3a-r** (0.4 mmol) in methanol (10 mL) was added portion-wise at 0 °C sodium borohydride (3.2 mmol, 8 eq.). The reaction mixture was then stirred at room temperature for 2 h. Then, it was evaporated to dryness under reduced pressure. After cooling, the residue was triturated in water and extracted with dichloromethane (40 mL). The organic layer was separated, dried over sodium sulfate and activated charcoal, and evaporated to dryness. The residue was then purified by column chromatography

on silica gel using dichloromethane/methanol (90/10: *v*/*v*) as eluent to give the pure products **4a-r**.

1,3,5-*Tris*[(4-(2-dimethylaminoethyl)aminomethyl)phenyl)methyl]benzene (**4a**)

Yellow oil (60%); ^{1}H NMR ($CDCl_3$) δ ppm: 7.23 (d, 6H, *J* = 8.10 Hz, H-3$_{phen}$ and H-5$_{phen}$), 7.11 (d, 6H, *J* = 8.10 Hz, H-2$_{phen}$ and H-6$_{phen}$), 6.86 (s, 3H, H$_{benz}$), 3.88 (s, 6H, CH_2), 3.78 (s, 6H, NCH_2), 2.70 (t, 6H, *J* = 6.90 Hz, NCH_2), 2.43 (t, 6H, *J* = 6.90 Hz, NCH_2), 2.21 (s, 18H, $N(CH_3)_2$); ^{13}C NMR ($CDCl_3$) δ ppm: 142.74 (C-4$_{phenyl}$), 141.17 (Cq$_{benz}$), 139.33 (C-1$_{phenyl}$), 130.24 (C-3$_{phen}$ and C-5$_{phen}$), 129.65 (C-2$_{phen}$ and C-6$_{phen}$), 128.81 (CH$_{benz}$), 60.43 (NCH_2), 55.17 (NCH_2), 48.02 (NCH_2), 46.91 ($N(CH_3)_2$), 42.84 (CH_2). ESI-MS m/z $[M+H]^+$ calculated for $C_{42}H_{61}N_6$: 649.4958, Found: 649.4952.

1,3,5-*Tris*[(4-(3-dimethylaminopropyl)aminomethyl)phenyl)methyl]benzene (**4b**)

Yellow oil (63%); ^{1}H NMR ($CDCl_3$) δ ppm: 7.22 (d, 6H, *J* = 8.10 Hz, H-3$_{phen}$ and H-5$_{phen}$), 7.11 (d, 6H, *J* = 8.10 Hz, H-2$_{phen}$ and H-6$_{phen}$), 6.86 (s, 3H, H$_{benz}$), 3.87 (s, 6H, CH_2), 3.76 (s, 6H, NCH_2), 2.68 (t, 6H, *J* = 7.10 Hz, NCH_2), 2.33 (t, 6H, *J* = 7.10 Hz, NCH_2), 2.22 (s, 18H, $N(CH_3)_2$), 1.69 (qt, 6H, *J* = 7.10 Hz, CH_2); ^{13}C NMR ($CDCl_3$) δ ppm: 142.70 (C-4$_{phenyl}$), 141.24 (Cq$_{benz}$), 139.16 (C-1$_{phenyl}$), 130.26 (C-3$_{phen}$ and C-5$_{phen}$), 129.61 (C-2$_{phen}$ and C-6$_{phen}$), 128.84 (CH$_{benz}$), 59.36 (NCH_2), 55.06 (NCH_2), 49.22 (NCH_2), 46.86 ($N(CH_3)_2$), 42.83 (CH_2), 29.19 (CH_2). ESI-MS m/z $[M+2H]^+$ calculated for $C_{45}H_{68}N_6$: 692.5505, found: 692.5491.

1,3,5-*Tris*[(4-(4-dimethylaminobutyl)aminomethyl)phenyl)methyl]benzene (**4c**)

Yellow oil (95%); ^{1}H NMR ($CDCl_3$) δ ppm: 7.20 (d, 6H, *J* = 7.90 Hz, H-3$_{phen}$ and H-5$_{phen}$), 7.08 (d, 6H, *J* = 7.90 Hz, H-2$_{phen}$ and H-6$_{phen}$), 6.84 (s, 3H, H$_{benz}$), 3.85 (s, 6H, CH_2), 3.73 (s, 6H, NCH_2), 2.64 (t, 6H, *J* = 6.90 Hz, NCH_2), 2.24 (t, 6H, *J* = 6.90 Hz, NCH_2), 2.18 (s, 18H, $N(CH_3)_2$), 1.53–1.48 (m, 12H, CH_2); ^{13}C NMR ($CDCl_3$) δ ppm: 142.71 (C-4$_{phenyl}$), 141.25 (Cq$_{benz}$), 139.23 (C-1$_{phenyl}$), 130.26 (C-3$_{phen}$ and C-5$_{phen}$), 129.63 (C-2$_{phen}$ and C-6$_{phen}$), 128.83 (CH$_{benz}$), 61.03 (NCH_2), 55.04 (NCH_2), 50.70 (NCH_2), 46.79 ($N(CH_3)_2$), 42.84 (CH_2), 29.29 (CH_2), 26.91 (CH_2). ESI-MS m/z $[M+H]^+$ calculated for $C_{48}H_{73}N_6$: 733.5896, found: 733.5887.

1,3,5-*Tris*[(4-(2-(4-methylpiperazin-1-yl)ethyl)aminomethyl)phenyl)methyl]benzene (**4d**)

Yellow oil (64%); ^{1}H NMR ($CDCl_3$) δ ppm: 7.21 (d, 6H, *J* = 8.10 Hz, H-3$_{phen}$ and H-5$_{phen}$), 7.10 (d, 6H, *J* = 8.10 Hz, H-2$_{phen}$ and H-6$_{phen}$), 6.85 (s, 3H, H$_{benz}$), 3.87 (s, 6H, CH_2), 3.76 (s, 6H, NCH_2), 2.70 (t, 6H, *J* = 6.90 Hz, NCH_2), 2.50 (t, 6H, *J* = 6.90 Hz, NCH_2), 2.48–2.35 (m, 24H, $NCH_{2piperazine}$), 2.27 (s, 9H, NCH_3); ^{13}C NMR ($CDCl_3$) δ ppm: 142.72 (C-4$_{phenyl}$), 141.17 (Cq$_{benz}$), 139.39 (C-1$_{phenyl}$), 130.21 (C-3$_{phen}$ and C-5$_{phen}$), 129.58 (C-2$_{phen}$ and C-6$_{phen}$), 128.82 (CH$_{benz}$), 59.07 (NCH_2), 56.51 ($NCH_{2piperazine}$), 55.07 (NCH_2), 54.52 ($NCH_{2piperazine}$), 47.43 (NCH_3), 47.04 (NCH_2), 42.83 (CH_2). ESI-MS m/z $[M+H]^+$ calculated for $C_{51}H_{76}N_9$: 814.6223, found: 814.6224.

1,3,5-*Tris*[(4-(3-(4-methylpiperazin-1-yl)propyl)aminomethyl)phenyl)methyl]benzene (**4e**)

Yellow oil (84%); ^{1}H NMR ($CDCl_3$) δ ppm: 7.18 (d, 6H, *J* = 8.10 Hz, H-3$_{phen}$ and H-5$_{phen}$), 7.06 (d, 6H, *J* = 8.10 Hz, H-2$_{phen}$ and H-6$_{phen}$), 6.82 (s, 3H, H$_{benz}$), 3.82 (s, 6H, CH_2), 3.71 (s, 6H, NCH_2), 2.64 (t, 6H, *J* = 7.10 Hz, NCH_2), 2.37 (t, 6H, *J* = 7.10 Hz, NCH_2), 2.41–2.34 (m, 24H, $NCH_{2piperazine}$), 2.23 (s, 9H, NCH_3), 1.67 (qt, 6H, *J* = 7.10 Hz, CH_2); ^{13}C NMR ($CDCl_3$) δ ppm: 142.61 (C-4$_{phenyl}$), 141.04 (Cq$_{benz}$), 139.26 (C-1$_{phenyl}$), 130.13 (C-3$_{phen}$ and C-5$_{phen}$), 129.48 (C-2$_{phen}$ and C-6$_{phen}$), 128.78 (CH$_{benz}$), 59.10 (NCH_2), 56.43 ($NCH_{2piperazine}$), 55.05 (NCH_2), 54.55 ($NCH_{2piperazine}$), 49.48 (NCH_2), 47.39 (NCH_3), 42.77 (CH_2), 28.20 (CH_2). ESI-MS m/z $[M+H]^+$ calculated for $C_{54}H_{82}N_9$: 856.6693, found: 856.6698.

1,3,5-*Tris*[(4-(3-(morpholin-1-yl)propyl)aminomethyl)phenyl)methyl]benzene (**4f**)

Yellow oil (50%); ^{1}H NMR ($CDCl_3$) δ ppm: 7.22 (d, 6H, *J* = 8.10 Hz, H-3$_{phen}$ and H-5$_{phen}$), 7.11 (d, 6H, *J* = 8.10 Hz, H-2$_{phen}$ and H-6$_{phen}$), 6.86 (s, 3H, H$_{benz}$), 3.88 (s, 6H, CH_2), 3.76 (s, 6H, NCH_2), 3.70 (t, 12H, *J* = 4.65 Hz, OCH_2), 2.69 (t, 6H, *J* = 6.90 Hz, NCH_2), 2.44 (t, 12H, *J* = 4.65 Hz, $NCH_{2\ morpholine}$), 2.39 (t, 6H, *J* = 6.90 Hz, NCH_2), 1.71 (qt, 6H, *J* = 6.90 Hz, CH_2); ^{13}C NMR ($CDCl_3$) δ ppm: 142.71 (C-4$_{phenyl}$), 141.21 (Cq$_{benz}$), 139.29 (C-1$_{phenyl}$), 130.24 (C-3$_{phen}$ and C-5$_{phen}$), 129.54 (C-2$_{phen}$ and C-6$_{phen}$), 128.82 (CH$_{benz}$), 68.33 (OCH_2),

58.74 (NCH_2), 55.14 ($NCH_{2morpholine}$), 49.38 (NCH_2), 42.82 (CH_2), 27.94 (CH_2). ESI-MS m/z $[M+H]^+$ calculated for $C_{51}H_{73}N_6O_3$: 817.5744, found: 817.5743.

1,3,5-*Tris*[(4-(3-(pyrrolidin-1-yl)propyl)aminomethyl)phenyl)methyl]benzene (**4g**)

Yellow oil (84%); ^1H NMR ($CDCl_3$) δ ppm: 7.18 (d, 6H, J = 8.10 Hz, H-3_{phen} and H-5_{phen}), 7.07 (d, 6H, J = 8.10 Hz, H-2_{phen} and H-6_{phen}), 6.83 (s, 3H, H_{benz}), 3.84 (s, 6H, CH_2), 3.73 (s, 6H, NCH_2), 2.65 (t, 6H, J = 6.90 Hz, NCH_2), 2.48–2.43 (m, 18H, NCH_2 and $NCH_{2pyrrolidine}$), 1.75–1.70 (m, 18H, CH_2 and $CH_{2pyrrolidine}$); ^{13}C NMR ($CDCl_3$) δ ppm: 142.70 (C-4_{phenyl}), 141.10 (Cq_{benz}), 139.42 (C-1_{phenyl}), 130.19 (C-3_{phen} and C-5_{phen}), 129.51 (C-2_{phen} and C-6_{phen}), 128.80 (CH_{benz}), 56.14 (NCH_2), 55.62 ($NCH_{2pyrrolidine}$), 55.06 (NCH_2), 49.48 (NCH_2), 42.82 (CH_2), 30.62 (CH_2), 24.78 ($CH_{2pyrrolidine}$). ESI-MS m/z $[M+H]^+$ calculated for $C_{51}H_{73}N_6$: 769.5896, found: 769.5881.

1,3,5-*Tris*[(4-(3-(piperidin-1-yl)propyl)aminomethyl)phenyl)methyl]benzene (**4h**)

Yellow oil (85%); ^1H NMR ($CDCl_3$) δ ppm: 7.20 (d, 6H, J = 8.10 Hz, H-3_{phen} and H-5_{phen}), 7.09 (d, 6H, J = 8.10 Hz, H-2_{phen} and H-6_{phen}), 6.84 (s, 3H, H_{benz}), 3.85 (s, 6H, CH_2), 3.73 (s, 6H, NCH_2), 2.66 (t, 6H, J = 6.90 Hz, NCH_2), 2.37–2.30 (m, 18H, NCH_2 and $NCH_{2piperidine}$), 1.70 (qt, 6H, J = 6.90 Hz, CH_2), 1.60–1.50 (m, 12H, $CH_{2piperidine}$), 1.44–1.40 (m, 6H, $CH_{2piperidine}$); ^{13}C NMR ($CDCl_3$) δ ppm: 142.69 (C-4_{phenyl}), 141.09 (Cq_{benz}), 139.40 (C-1_{phenyl}), 130.19 (C-3_{phen} and C-5_{phen}), 129.51 (C-2_{phen} and C-6_{phen}), 128.79 (CH_{benz}), 59.16 (NCH_2), 56.04 (NCH_2 $_{piperidine}$), 55.05 (NCH_2), 49.66 (NCH_2), 42.82 (CH_2), 28.36 (CH_2), 27.35 ($CH_{2piperidine}$), 25.83 ($CH_{2piperidine}$). ESI-MS m/z $[M+H]^+$ calculated for $C_{54}H_{79}N_6$: 811.6366, found: 811.6358.

1,3,5-*Tris*[(4-((quinolin-3-yl)aminomethyl)phenyl)methyl]benzene (**4i**)

Pale-yellow crystals (33%); M.p. = 135 °C; ^1H NMR ($CDCl_3$) δ ppm: 8.48 (d, 3H, J = 2.70 Hz, H-2_{quinol}), 7.95 (dd, 3H, J = 6.90 and 3.60 Hz, H-8_{quinol}), 7.59 (dd, 3H, J = 6.90 and 3.60 Hz, H-5_{quinol}), 7.44–7.39 (m, 6H, H-6_{quinol} and H-7_{quinol}), 7.29 (d, 6H, J = 7.80 Hz, H-3_{phen} and H-5_{phen}), 7.15 (d, 6H, J = 7.80 Hz, H-2_{phen} and H-6_{phen}), 7.03 (d, 3H, J = 2.70 Hz, H-4_{quinol}), 6.89 (s, 3H, H_{benz}), 3.91 (s, 6H, CH_2); ^{13}C NMR ($CDCl_3$) δ ppm: 144.62 (C-2_{quinol}), 143.50 (C-$8a_{quinol}$), 142.67 (C-4_{phenyl} and C-3_{quinol}), 141.93 (Cq_{benz}), 137.23 (C-1_{phenyl}), 134.93 (C-$4a_{quinol}$), 130.61 (C-3_{phen} and C-5_{phen}), 130.35 (C-4_{quinol}), 129.02 (C-2_{phen} and C-6_{phen}), 129.00 (C-8_{quinol}), 128.33 (CH_{benz}), 127.37 (C-6_{quinol}), 126.40 (C-7_{quinol}), 111.82 (C-5_{quinol}), 49.03 (NCH_2), 42.82 (CH_2). ESI-MS m/z $[M+H]^+$ calculated for $C_{57}H_{49}N_6$: 817.4018, found: 817.4009.

1,3,5-*Tris*[(4-(pyridin-2-ylmethylaminomethyl)phenyl)methyl]benzene (**4j**)

Yellow oil (62%); ^1H NMR ($CDCl_3$) δ ppm: 8.57–8.55 (m, 3H, H-6_{pyrid}), 7.66–7.62 (m, 3H, H-4_{pyrid}), 7.33–7.25 (m, 9H, H-3_{phen}, H-5_{phen}, and H-3_{pyrid}), 7.19–7.10 (m, 9H, H-6_{phen}, H-2_{phen}, and H-5_{pyrid}), 6.87 (s, 3H, H_{benz}), 3.94 (s, 6H, NCH_2), 3.88 (s, 6H, CH_2), 3.82 (s, 6H, NCH_2); ^{13}C NMR ($CDCl_3$) δ ppm: 161.00 (C-2_{pyrid}), 150.66 (C-6_{pyrid}), 142.74 (C-4_{phenyl}), 141.31 (Cq_{benz}), 138.97 (C-1_{phenyl}), 137.84 (C-4_{pyrid}), 130.28 (C-3_{phen} and C-5_{phen}), 129.78 (C-2_{phen} and C-6_{phen}), 128.83 (CH_{benz}), 123.77 (C-3_{pyrid}), 123.35 (C-5_{pyrid}), 55.80 (NCH_2), 54.53 (NCH_2), 42.85 (CH_2). ESI-MS m/z $[M+H]^+$ calculated for $C_{48}H_{49}N_6$: 709.4018, found: 709.4010.

1,3,5-*Tris*[(4-(pyridin-2-ylethylaminomethyl)phenyl)methyl]benzene (**4k**)

Yellow oil (96%); ^1H NMR ($CDCl_3$) δ ppm: 8.51–8.49 (m, 3H, H-6_{pyrid}), 7.56–7.50 (m, 3H, H-4_{pyrid}), 7.20–7.11 (m, 9H, H-3_{phen}, H-5_{phen}, and H-3_{pyrid}), 7.09–7.05 (m, 9H, H-6_{phen}, H-2_{phen}, and H-5_{pyrid}), 6.84 (s, 3H, H_{benz}), 3.83 (s, 6H, NCH_2), 3.77 (s, 6H, CH_2), 3.05–2.97 (m, 12H, NCH_2 and CH_2Pyrid); ^{13}C NMR ($CDCl_3$) δ ppm: 161.63 (C-2_{pyrid}), 150.66 (C-6_{pyrid}), 142.72 (C-4_{phenyl}), 141.14 (Cq_{benz}), 139.33 (C-1_{phenyl}), 137.70 (C-4_{pyrid}), 130.21 (C-3_{phen} and C-5_{phen}), 129.57 (C-2_{phen} and C-6_{phen}), 128.76 (CH_{benz}), 124.65 (C-3_{pyrid}), 122.60 (C-5_{pyrid}), 54.93 (NCH_2), 50.24 (NCH_2), 42.83 (CH_2), 39.80 (CH_2). ESI-MS m/z $[M+H]^+$ calculated for $C_{51}H_{55}N_6$: 751.4488, found: 751.4474.

1,3,5-*Tris*[(4-(pyridin-2-ylpropylaminomethyl)phenyl)methyl]benzene (**4l**)

Yellow oil (78%); ^1H NMR ($CDCl_3$) δ ppm: 8.48–8.45 (m, 3H, H-6_{pyrid}), 7.55–7.48 (m, 3H, H-4_{pyrid}), 7.18 (d, 6H, J = 8.10 Hz, H-3_{phen} and H-5_{phen}), 7.11–7.01 (m, 12H, H-6_{phen}, H-2_{phen}, H-5_{pyrid}, and H-3_{pyrid}), 6.84 (s, 3H, H_{benz}), 3.84 (s, 6H, NCH_2), 3.71 (s, 6H, CH_2),

2.81 (t, 6H, *J* = 6.90 Hz, NCH_2), 2.66 (t, 6H, *J* = 6.90 Hz, CH_2Pyrid), 1.92 (qt, *J* = 6.90 Hz, CH_2); ^{13}C NMR ($CDCl_3$) δ ppm: 163.09 (C-2_{pyrid}), 150.45 (C-6_{pyrid}), 142.72 (C-4_{phenyl}), 141.20 (Cq_{benz}), 139.25 (C-1_{phenyl}), 137.79 (C-4_{pyrid}), 130.22 (C-3_{phen} and C-5_{phen}), 129.62 (C-2_{phen} and C-6_{phen}), 128.81 (CH_{benz}), 124.18 (C-3_{pyrid}), 122.43 (C-5_{pyrid}), 54.92 (NCH_2), 50.06 (NCH_2), 42.83 (CH_2), 37.26 (CH_2), 31.37 (CH_2). ESI-MS m/z $[M+H]^+$ calculated for $C_{54}H_{61}N_6$: 793.4957, found: 793.4941.

1,3,5-*Tris*[(4-(pyridin-3-ylmethylaminomethyl)phenyl)methyl]benzene (**4m**)

Pale-yellow oil (70%); ^{1}H NMR ($CDCl_3$) δ ppm: 8.57–8.48 (m, 6H, H-6_{pyrid} and H-3_{pyrid}), 7.69 (d, 3H, *J* = 7.80 Hz, H-4_{pyrid}), 7.28–7.24 (m, 3H, H-5_{pyrid}), 7.23 (d, 6H, *J* = 8.10 Hz, H-3_{phen} and H-5_{phen}), 7.12 (d, 6H, *J* = 8.10 Hz, H-6_{phen} and H-2_{phen}), 6.88 (s, 3H, H_{benz}), 3.88 (s, 6H, NCH_2), 3.79 (s, 6H, NCH_2), 3.76 (s, 6H, CH_2); ^{13}C NMR ($CDCl_3$) δ ppm: 151.05 (C-2_{pyrid}), 149.78 (C-6_{pyrid}), 142.72 (C-4_{phenyl}), 141.44 (Cq_{benz}), 138.89 (C-1_{phenyl}), 137.29 (C-4_{pyrid}), 137.02 (C-3_{pyrid}), 130.32 (C-3_{phen} and C-5_{phen}), 129.63 (C-2_{phen} and C-6_{phen}), 128.87 (CH_{benz}), 124.83 (C-5_{pyrid}), 54.26 (NCH_2), 51.79 (NCH_2), 42.86 (CH_2). ESI-MS m/z $[M+H]^+$ calculated for $C_{48}H_{49}N_6$: 709.4018, found: 709.4007.

1,3,5-*Tris*[(4-(pyridin-3-ylethylaminomethyl)phenyl)methyl]benzene (**4n**)

Yellow oil (90%); ^{1}H NMR ($CDCl_3$) δ ppm: 8.45–8.39 (m, 6H, H-6_{pyrid} and H-3_{pyrid}), 7.47 (d, 3H, *J* = 7.80 Hz, H-4_{pyrid}), 7.20–7.17 (m, 3H, H-5_{pyrid}), 7.16 (d, 6H, *J* = 7.80 Hz, H-3_{phen} and H-5_{phen}), 7.07 (d, 6H, *J* = 7.80 Hz, H-6_{phen} and H-2_{phen}), 6.84 (s, 3H, H_{benz}), 3.83 (s, 6H, NCH_2), 3.74 (s, 6H, CH_2), 2.91–2.75 (m, 12H, NCH_2 and CH_2Pyrid); ^{13}C NMR ($CDCl_3$) δ ppm: 151.38 (C-2_{pyrid}), 148.90 (C-6_{pyrid}), 142.67 (C-4_{phenyl}), 141.31 (Cq_{benz}), 138.95 (C-1_{phenyl}), 137.61 (C-4_{pyrid}), 136.75 (C-3_{pyrid}), 130.25 (C-3_{phen} and C-5_{phen}), 129.56 (C-2_{phen} and C-6_{phen}), 128.82 (CH_{benz}), 124.77 (C-5_{pyrid}), 54.83 (NCH_2), 51.43 (NCH_2), 42.80 (CH_2), 34.83 (CH_2). ESI-MS m/z $[M+H]^+$ calculated for $C_{51}H_{55}N_6$: 751.4488, found: 751.4474.

1,3,5-*Tris*[(4-(pyridin-3-ylpropylaminomethyl)phenyl)methyl]benzene (**4o**)

Yellow oil (98%); ^{1}H NMR ($CDCl_3$) δ ppm: 8.44–8.41 (m, 6H, H-6_{pyrid} and H-3_{pyrid}), 7.44 (d, 3H, *J* = 7.80 Hz, H-4_{pyrid}), 7.20 (d, 6H, *J* = 8.10 Hz, H-3_{phen} and H-5_{phen}), 7.19–7.13 (m, 3H, H-5_{pyrid}), 7.09 (d, 6H, *J* = 8.10 Hz, H-6_{phen} and H-2_{phen}), 6.86 (s, 3H, H_{benz}), 3.86 (s, 6H, NCH_2), 3.72 (s, 6H, CH_2), 2.67–2.60 (m, 12H, NCH_2 and CH_2Pyrid), 1.80 (qt, 6H, *J* = 7.20 Hz, CH_2); ^{13}C NMR ($CDCl_3$) δ ppm: 151.16 (C-2_{pyrid}), 148.60 (C-6_{pyrid}), 142.71 (C-4_{phenyl}), 141.26 (Cq_{benz}), 139.27 (C-1_{phenyl}), 138.76 (C-3_{pyrid}), 137.24 (C-4_{pyrid}), 130.25 (C-3_{phen} and C-5_{phen}), 129.61 (C-2_{phen} and C-6_{phen}), 128.84 (CH_{benz}), 124.71 (C-5_{pyrid}), 55.05 (NCH_2), 49.94 (NCH_2), 42.83 (CH_2), 32.71 (CH_2), 32.00 (CH_2). ESI-MS m/z $[M+H]^+$ calculated for $C_{54}H_{61}N_6$: 793.4957, found: 793.4941.

1,3,5-*Tris*[(4-(pyridin-4-ylmethylaminomethyl)phenyl)methyl]benzene (**4p**)

Yellow oil (78%); ^{1}H NMR ($CDCl_3$) δ ppm: 8.54 (d, 6H, *J* = 6.00 Hz, H-2_{pyrid} and H-6_{pyrid}), 7.30–7.23 (m, 12H, H-3_{pyrid}, H-5_{pyrid}, H-3_{phen}, and H-5_{phen}), 7.14 (d, 6H, *J* = 8.10 Hz, H-6_{phen} and H-2_{phen}), 6.89 (s, 3H, H_{benz}), 3.90 (s, 6H, NCH_2), 3.82 (s, 6H, NCH_2), 3.77 (s, 6H, CH_2); ^{13}C NMR ($CDCl_3$) δ ppm: 151.15 (C-2_{pyrid} and C-6_{pyrid}), 150.6 (C-4_{pyrid}), 142.71 (C-4_{phenyl}), 141.48 (Cq_{benz}), 138.84 (C-1_{phenyl}), 130.32 (C-3_{phen} and C-5_{phen}), 129.62 (C-2_{phen} and C-6_{phen}), 128.91 (CH_{benz}), 124.39 (C-3_{pyrid} and C-5_{pyrid}), 54.28 (NCH_2), 53.21 (NCH_2), 42.86 (CH_2). ESI-MS m/z $[M+H]^+$ calculated for $C_{48}H_{49}N_6$: 709.4018, found: 709.4018.

1,3,5-*Tris*[(4-(pyridin-4-ylethylaminomethyl)phenyl)methyl]benzene (**4q**)

Yellow oil (86%); ^{1}H NMR ($CDCl_3$) δ ppm: 8.52–8.49 (m, 6H, H-2_{pyrid} and H-6_{pyrid}), 7.19 (d, 6H, *J* = 8.10 Hz, H-3_{phen} and H-5_{phen}), 7.10–7.07 (m, 12H, H-3_{pyrid}, H-5_{pyrid}, H-6_{phen} and H-2_{phen}), 6.87 (s, 3H, H_{benz}), 3.87 (s, 6H, NCH_2), 3.77 (s, 6H, CH_2), 2.92 (t, 6H, *J* = 6.90 Hz, NCH_2), 2.80 (t, 6H, *J* = 6.90 Hz, CH_2); ^{13}C NMR ($CDCl_3$) δ ppm: 151.16 (C-2_{pyrid} and C-6_{pyrid}), 150.54 (C-4_{pyrid}), 142.72 (C-4_{phenyl}), 141.34 (Cq_{benz}), 139.05 (C-1_{phenyl}), 130.29 (C-3_{phen} and C-5_{phen}), 129.57 (C-2_{phen} and C-6_{phen}), 128.87 (CH_{benz}), 125.57 (C-3_{pyrid} and C-5_{pyrid}), 54.91 (NCH_2), 50.75 (NCH_2), 42.85 (CH_2), 37.13 (CH_2). ESI-MS m/z $[M+H]^+$ calculated for $C_{51}H_{55}N_6$: 751.4488, found: 751.4475.

1,3,5-*Tris*[(4-(pyridin-4-ylpropylaminomethyl)phenyl)methyl]benzene (**4r**)

Yellow oil (49%); ^{1}H NMR ($CDCl_3$) δ ppm: 8.45 (d, 6H, *J* = 6.00 Hz, H-2_{pyrid} and H-6_{pyrid}), 7.19 (d, 6H, *J* = 8.10 Hz, H-3_{phen} and H-5_{phen}), 7.09 (d, 6H, *J* = 8.10 Hz, H-6_{phen}

and H-2_{phen}), 7.08–7.05 (m, 6H, H-3_{pyrid} and H-5_{pyrid}), 6.86 (s, 3H, H_{benz}), 3.86 (s, 6H, NCH_2), 3.72 (s, 6H, CH_2), 2.64 (t, 12H, J = 7.20 Hz, NCH_2 and CH_2Pyrid), 1.80 (qt, 6H, J = 7.20 Hz, CH_2); ^{13}C NMR ($CDCl_3$) δ ppm: 152.20 (C-4_{pyrid}), 151.02 (C-2_{pyrid} and C-6_{pyrid}), 142.71 (C-4_{phenyl}), 141.36 (Cq_{benz}), 139.11 (C-1_{phenyl}), 130.29 (C-3_{phen} and C-5_{phen}), 129.64 (C-2_{phen} and C-6_{phen}), 128.88 (CH_{benz}), 125.28 (C-3_{pyrid} and C-5_{pyrid}), 55.02 (NCH_2), 49.93 (NCH_2), 42.85 (CH_2), 34.24 (CH_2), 31.09 (CH_2). ESI-MS m/z $[M+H]^+$ calculated for $C_{54}H_{61}N_6$: 793.4957, found: 793.4958.

3.2. Biological Evaluation

3.2.1. In Vitro Antiplasmodial Activity

Derivatives **1** were dissolved in DMSO and then diluted in sterile water in order to obtain a range of concentration from 40 nM to 40 mM for the first screening against culture-adapted *Plasmodium falciparum* reference strains, 3D7 and W2. The former strain is susceptible to chloroquine (CQ) but displays a decreased susceptibility to mefloquine (MQ); the latter is considered resistant to CQ. These two strains were obtained from the collection of the National Museum of Natural History (Paris, France). The parasites were cultivated in RPMI medium (Sigma-Aldrich, Lyon, France) supplemented with 0.5% Albumax I (Life Technologies Corporation, Paisley, UK), hypoxanthine (Sigma-Aldrich), and gentamicin (Sigma-Aldrich) with human erythrocytes and were incubated at 37 °C in a candle jar, as described previously [32]. The *P. falciparum* drug susceptibility test was carried out in 96-well flat-bottom sterile plates in a final volume of 250 µL. After 48 h incubation period with the drugs, quantities of DNA in treated and control cultures of parasites in human erythrocytes were quantified using the SYBR Green I (Sigma-Aldrich) fluorescence-based method [33,34]. Briefly, after incubation, plates were frozen at -20 °C until use. Plates were then thawed for 2 h at room temperature, and 100 µL of each homogenized culture was transferred to a well of a 96-well flat-bottom sterile black plate (Sigma-Aldrich, Lyon, France) that contained 100 µL of the SYBR Green I lysis buffer (2xSYBR Green, 20 mM Tris base pH 7.5, 5 mM EDTA, 0.008% *w*/*v* saponin, 0.08% *w*/*v* Triton X-100). Negative controls treated with solvent (typically DMSO or H_2O) and positive controls (CQ and MQ) were added to each set of experiments. Plates were incubated for 1 h at room temperature and then read on a fluorescence plate reader (Tecan Trading AG, Männedorf, Switzerland) using excitation and emission wavelengths of 485 and 535 nm, respectively. The concentrations at which the screening drug or antimalarial is capable of inhibiting 50% of parasitic growth (IC_{50}) were calculated from a sigmoid inhibition model Emax with an estimate of IC_{50} by non-linear regression (IC Estimator version 1.2) and were reported as means calculated from three independent experiments [35].

3.2.2. In Vitro Antileishmanial Activity

L. donovani (MHOM/IN/00/DEVI) used in this study was provided by the CNR Leishmania (Montpellier, France). The effects of the tested compounds on the growth of *L. donovani* (MHOM/IN/00/DEVI) promastigotes were assessed by MTT assay [36]. Briefly, promastigotes in log phase in Schneider's medium supplemented with 20% fetal calf serum (FCS), 2 mM L-glutamine, and antibiotics (100 U/mL penicillin and 100 µg/mL streptomycin) were incubated at an average density of 10^6 parasites/mL in sterile 96-well plates with various concentrations of compounds previously dissolved in DMSO (final concentration less than 0.5% *v*/*v*), in duplicate. Appropriate controls treated with DMSO, pentamidine, and amphotericin B (reference drugs purchased from Sigma-Aldrich) were added to each set of experiments. Duplicate assays were performed for each sample. After a 72 h incubation period at 27 °C, parasite metabolic activity was determined. Each well was microscopically examined for precipitate formation. To each well was added 10 µL of 10 mg/mL MTT (3-(4,5-dimethylthiazol-2-yl)-2,5-diphenyltetrazolium bromide) solution followed by 4 h incubation time. The enzyme reaction was stopped by addition of 100 µL of 50% isopropanol/10% sodium dodecyl sulfate [37]. Plates were vigorously shaken (300 rpm) for 10 min, and the absorbance was measured at 570 nm with 630 nm as reference

wavelength in a BIO-TEK ELx808 Absorbance Microplate Reader (Agilent Technologies, Les Ulis, France). The IC_{50} was defined as the concentration of drug required to inhibit by 50% of the metabolic activity of *L. donovani* promastigotes compared to the control. IC_{50} of the parasite's growth (half maximal inhibitory concentration or IC_{50} values) were then calculated from the obtained experimental results using a previously described regression program [35]. IC_{50} values were calculated from three independent experiments.

3.2.3. Cytotoxicity Evaluation

A cytotoxicity evaluation was performed using the method reported by Mosmann [36] with slight modifications to determine the cytotoxic concentrations 50% (CC_{50}) and using doxorubicin as a cytotoxic reference compound. These assays were performed in human HepG2 cells purchased from ATCC (ref HB-8065). These cells are a commonly used human hepatocarcinoma-derived cell line that has characteristics similar to those of primary hepatocytes. These cells express many hepatocyte-specific metabolic enzymes, thus enabling the cytotoxicity of tested product metabolites to be evaluated. Briefly, cells in 100 µL of complete RPMI medium (RPMI supplemented with 10% FCS, 1% L-glutamine (200 mM), penicillin (100 U/mL), and streptomycin (100 µg/mL)) were inoculated at 37 °C into each well of 96-well plates in a humidified chamber in 6% CO_2. After 24 h, 100 µL of medium with the test compound at various concentrations dissolved in DMSO (final concentration less than 0.5% *v*/*v*) were added, and the plates were incubated for 72 h at 37 °C. Duplicate assays were performed for each sample. Each well was microscopically examined for precipitate formation before the medium was aspirated from the wells. After aspiration, 100 µL of MTT solution (0.5 mg/mL in medium without FCS) was then added to each well. Cells were incubated for 2 h at 37 °C. The MTT solution was removed, and DMSO (100 µL) was added to dissolve the resulting blue formazan crystals. Plates were shaken vigorously (300 rpm) for 5 min. The absorbance was measured at 570 nm with 630 nm as the reference wavelength in a BIO-TEK ELx808 Absorbance Microplate Reader. DMSO was used as blank and doxorubicin (Sigma Aldrich) as the positive control. Cell viability was calculated as percentage of control (cells incubated without compound). The CC_{50} was determined from the dose–response curve using TableCurve 2D V5.0 software (Systat Software, Palo Alto, CA, USA).

3.3. FRET Melting Experiments

Some bioactive compounds **1** were selected for the subsequent FRET melting experiments. These were performed with dual-labeled oligonucleotides mimicking the *Plasmodium* telomeric sequences FPf1T (FAM-5′(GGGTTTA)3-GGG3′-TAMRA) and FPf8T [FAM-5′(GGGTTCA)3GGG3′-TAMRA], the human telomeric sequence F21T (FAM-(GGGTTA)3-GGG3′-TAMRA), and the human duplex sequence FdxT (FAM5′-TATAGCTATA-hexaethyleneglycol-TATAGCTATA3′-TAMRA) [14,17,38]. The oligonucleotides were pre-folded in 10 mM lithium cacodylate buffer (pH 7.2), with 10 mM KCl and 90 mM LiCl (K+ condition). The FAM emissions were recorded at 516 nm using a 492 nm excitation wavelength in the absence and presence of a single compound as a function of temperature (25 to 95 °C) in 96-well microplates by using a Stratagene MX3000P real-time PCR device at a rate of 1 °C·min^{-1}. Data were normalized between 0 and 1, and the required temperature for half denaturation of oligonucleotides corresponding to an emission value of 0.5 was taken as the Tm. Each experiment was performed in duplicate with 0.2 µM of labeled oligonucleotide and 2 µM of compound under K^+ condition. For each compound, three independent experiments were carried out.

4. Conclusions

In the present research report, we described the synthesis, the antimalarial potentialities, and the *in vitro* cytotoxicity toward human cells of a new and original series of 1,3,5-*tris*[(4-(substituted-aminomethyl)phenyl)methyl]benzene derivatives **1**. These new derivatives were tested for their *in vitro* antiprotozoal activity toward the CQ-resistant

W2 and CQ-sensitive 3D7 *P. falciparum* strains and the promastigote form of *L. donovani*. In addition, the *in vitro* cytotoxicity of these new original aza and polyaromatic compounds was assessed on the human HepG2 cell line. Among these new synthesized nitrogen polyaromatic molecules, some of them were found as interesting potential in vitro antiplasmodial leads with IC_{50} values in the sub and μM range against the W2 and 3D7 strains of *P. falciparum*. Particularly, compounds **1m-n** and **1r** were found to be the most active derivatives against the 3D7 strain, whereas **1r** presented the best antiprotozoal activities against both *Plasmodium* W2 and 3D7 strains. Interestingly, 1,3,5-*tris*[(4-(substituted-aminomethyl)phenyl)methyl]benzene **1m** was identified as the most potent and promising antimalarial candidate with a ratio of cytotoxic to antiparasitic activities of 83.67 against the *P. falciparum* CQ-sensitive strain 3D7. In addition, we can also remark that most of our new synthesized derivatives **1** were found more active against the CQ-sensitive and MQ decreased sensitivity strain 3D7 than against the CQ-resistant and mefloquine-sensitive *P. falciparum* strain W2. Moreover, three 1,3,5-*tris*[(4-(substituted-aminomethyl)phenyl)methyl]benzenes showed moderate activity against the promastigote forms of *L. donovani*, with IC_{50} data ranging from 5.96 to 14.04 μM. As the telomeres of the various parasites could constitute interesting and potential targets, we have also investigated the possibility of targeting *Plasmodium* telomeres by stabilizing the *Plasmodium* G-quadruplex sequences using FRET melting assays with our new synthesized compounds. With regard to the stabilization of the protozoal G-quadruplex, it could be noticed that the best 1,3,5-*tris*[(4-(substituted-aminomethyl)phenyl)methyl]benzenes **1**, which exhibited an interesting stabilization profile, were not the most bioactive compounds against *Plasmodium*. Thus, we have not found any correlations between the antimalarial activity and selectivity of these novel compounds and their respective binding to G-quadruplexes. These 1,3,5-*tris*[(4-(substituted-aminomethyl)phenyl)methyl]benzene derivatives are, therefore, unlikely to be specifically cytotoxic via G-quadruplex binding. Moreover, it would be now interesting to enlarge the pharmacological evaluation of our novel 1,3,5-*tris*[(4-(substituted-aminomethyl)phenyl)methyl]benzene derivatives **1** by studying their potential mechanism of action by using further investigations such as the inhibition of beta-hematin formation or apicoplast functions. In conclusion, the new polyaromatic 1,3,5-*tris*[(4-(substituted-aminomethyl)phenyl)methyl]benzenes could open the way to new potential valuable and original medicinal chemistry scaffolding in the antimalarial domain.

Author Contributions: J.G., S.A.-R., S.M (Stéphane Moreau)., P.S. and J.-L.M. performed the synthesis and prepared and revised the manuscript; S.A.-R., J.G. and S.S. carried out the experiments; S.A.-R., I.K. and L.R. helped in the analysis of the compounds; A.C., S.M. (Serge Moukha), P.D., P.A. and P.S. conducted the *in vitro* tests. All authors have read and agreed to the published version of the manuscript.

Funding: This research received no external funding.

Institutional Review Board Statement: Not applicable.

Informed Consent Statement: Not applicable.

Data Availability Statement: Not applicable.

Acknowledgments: The authors would like to thank Philippe Grellier, department RDDM at Muséum National d'Histoire Naturelle (Paris, France), for generously providing the 3D7 and W2 *P. falciparum* strains.

Conflicts of Interest: The authors report no conflicts of interest. The authors alone are responsible for the content and writing of the paper.

References

1. WHO Guidelines for Malaria, Geneva: World Health Organization; 2022 (WHO/UCN/GMP/2022.01 Rev.2). License: CC BY-NC-SA 3.0 IGO. Available online: https://apps.who.int/iris/handle/10665/354781 (accessed on 6 March 2023).
2. WHO Guidelines for Malaria Hosted on the MAGICapp Online Platform. Available online: https://app.magicapp.org/#/guideline/7089 (accessed on 6 March 2023).

3. World Malaria Report 2022. Available online: https://www.who.int/teams/global-malaria-programme/reports/world-malaria-report-2022 (accessed on 5 March 2023).
4. WHO Neglected Tropical Diseases. Available online: https://www.who.int/news-room/questions-and-answers/item/neglected-tropical-diseases (accessed on 5 March 2023).
5. WHO Ending the Neglect to Attain the Sustainable Development Goals: A Rationale for Continued Investment in Tackling Neglected Tropical Diseases 2021–2030. Available online: https://www.who.int/publications/i/item/9789240052932 (accessed on 5 March 2023).
6. Dola, V.R.; Soni, A.; Agarwal, P.; Ahmad, H.; Raju, K.S.R.; Rashid, M.; Wahajuddin, M.; Srivastava, K.; Haq, W.; Dwivedi, A.K.; et al. Synthesis and Evaluation of Chirally Defined Side Chain Variants of 7-Chloro-4-Aminoquinoline to Overcome Drug Resistance in Malaria Chemotherapy. *Antimicrob. Agents Chemother.* **2017**, *61*, e01152-16. [CrossRef] [PubMed]
7. Manohar, S.; Tripathi, M.; Rawat, D.S. 4-Aminoquinoline based molecular hybrids as antimalarials: An overview. *Curr. Top. Med. Chem.* **2014**, *14*, 1706–1733. [CrossRef] [PubMed]
8. Deshpande, S.; Kay, B. 4-aminoquinolines: An Overview of Antimalarial Chemotherapy. *Med. Chem.* **2016**, *6*, 1. [CrossRef]
9. Kumar, S.; Singh, R.K.; Patial, B.; Goyal, S.; Bhardwaj, T.R. Recent advances in novel heterocyclic scaffolds for the treatment of drug-resistant malaria. *J. Enzyme Inhib. Med. Chem.* **2016**, *31*, 173–186. [CrossRef]
10. Van de Walle, T.; Cools, L.; Mangelinckx, S.; D'hooghe, M. Affiliations expand et al. Recent contributions of quinolines to antimalarial and anticancer drug discovery research. *Eur. J. Med. Chem.* **2021**, *226*, 113865. [CrossRef]
11. Goyal, A.; Kharkwal, H.; Piplani, M.; Singh, Y.; Murugesan, S.; Aggarwal, A.; Kumar, P.; Chander, S. Spotlight on 4-substituted quinolines as potential anti-infective agents: Journey beyond chloroquine. *Arch. Pharm.* **2023**, *356*, e2200361. [CrossRef]
12. Guillon, J.; Grellier, P.; Labaied, M.; Sonnet, P.; Léger, J.-M.; Déprez-Poulain, R.; Forfar-Bares, I.; Dallemagne, P.; Lemaître, N.; Péhourcq, F.; et al. Synthesis, antimalarial activity, and molecular modeling of new pyrrolo[1,2-*a*]quinoxalines, bispyrrolo[1,2-*a*]quinoxalines, bispyrido[3,2-*e*]pyrrolo[1,2-*a*]pyrazines, and bispyrrolo[1,2-a]thieno[3,2-*e*]pyrazines. *J. Med. Chem.* **2004**, *47*, 1997–2009. [CrossRef] [PubMed]
13. Dassonville-Klimpt, A.; Cézard, C.; Mullié, C.; Agnamey, P.; Jonet, A.; Da Nascimento, S.; Marchivie, M.; Guillon, J.; Sonnet, P. Absolute Configuration and Antimalarial Activity of erythro-Mefloquine Enantiomers. *ChemPlusChem* **2013**, *78*, 642–646. [CrossRef]
14. Guillon, J.; Cohen, A.; Gueddouda, N.M.; Das, R.N.; Moreau, S.; Ronga, L.; Savrimoutou, S.; Basmaciyan, L.; Monnier, A.; Monget, M.; et al. Design, synthesis and antimalarial activity of novel bis{*N*-[(pyrrolo[1,2-*a*]quinoxalin-4-yl)benzyl]-3-aminopropyl}amine derivatives. *J. Enzyme Inhib. Med. Chem.* **2017**, *32*, 547–563. [CrossRef]
15. Jonet, A.; Guillon, J.; Mullie, C.; Cohen, A.; Bentzinger, G.; Schneider, J.; Taudon, N.; Hutter, S.; Azas, N.; Moreau, S.; et al. Synthesis and Antimalarial Activity of New Enantiopure Aminoalcoholpyrrolo[1,2-*a*]quinoxalines. *Med. Chem.* **2018**, *14*, 293–303. [CrossRef]
16. Dassonville-Klimpt, A.; Schneider, J.; Damiani, C.; Tisnerat, C.; Cohen, A.; Azas, N.; Marchivie, M.; Guillon, J.; Mullié, C.; Agnamey, P.; et al. Design, synthesis, and characterization of novel aminoalcohol quinolines with strong *in vitro* antimalarial activity. *Eur. J. Med. Chem.* **2022**, *228*, 113981. [CrossRef]
17. Guillon, J.; Cohen, A.; Nath Das, R.; Boudot, C.; Meriem Gueddouda, N.; Moreau, S.; Ronga, L.; Savrimoutou, S.; Basmaciyan, L.; Tisnerat, C.; et al. Design, synthesis, and antiprotozoal evaluation of new 2,9-bis[(substituted-aminomethyl)phenyl]-1,10-phenanthroline derivatives. *Chem. Biol. Drug Des.* **2018**, *91*, 974–995. [CrossRef]
18. Guillon, J.; Cohen, A.; Monic, S.; Boudot, C.; Savrimoutou, S.; Albenque-Rubio, S.; Moreau, S.; Dassonville-Klimpt, A.; Mergny, J.-L.; Ronga, L.; et al. Synthesis and antiprotozoal evaluation of new 2,9-bis[(pyridinylalkylaminomethyl)phenyl]-1,10-phenanthroline derivatives by targeting G-quadruplex, an interesting pharmacophore against drug efflux. *Acta Sci. Pharm. Sci.* **2023**, *7*, 50–65. [CrossRef]
19. Guillon, J.; Cohen, A.; Boudot, C.; Monic, S.; Savrimoutou, S.; Moreau, S.; Albenque-Rubio, S.; Lafon-Schmaltz, C.; Dassonville-Klimpt, A.; Mergny, J.-L.; et al. Design, synthesis, biophysical and antiprotozoal evaluation of new promising 2,9-bis[(substituted-aminomethyl)]-4,7-phenyl-1,10-phenanthroline derivatives by targeting G-quadruplex, a potential alternative to drug efflux. *Pathogens* **2022**, *11*, 1339. [CrossRef] [PubMed]
20. Guillon, J.; Cohen, A.; Boudot, C.; Valle, A.; Milano, V.; Das, R.N.; Guédin, A.; Moreau, S.; Ronga, L.; Savrimoutou, S.; et al. Design, synthesis, and antiprotozoal evaluation of new 2,4-bis[(substituted-aminomethyl)phenyl]quinoline, 1,3-bis[(substituted-aminomethyl)phenyl]isoquinoline and 2,4-bis[(substituted-aminomethyl)phenyl]quinazoline derivatives. *J. Enzyme Inhib. Med. Chem.* **2020**, *35*, 432–459. [CrossRef]
21. Calvo, E.P.; Wasserman, M. G-Quadruplex ligands: Potent inhibitors of telomerase activity and cell proliferation in *Plasmodium falciparum*. *Mol. Biochem. Parasitol.* **2016**, *207*, 33–38. [CrossRef]
22. Tidwell, R.R.; Boykin, D.W.; Ismail, M.A.; Wilson, W.D.; White, E.W.; Kumar, A.; Nanjunda, R. Dicationic Compounds which Selectively Recognize G-quadruplex DNA. EP 1792613A2, 6 June 2007.
23. Leeder, W.-M.; Hummel, N.F.C.; Göringer, H.U. Multiple G-quartet structures in pre-edited mRNAs suggest evolutionary driving force for RNA editing in trypanosomes. *Sci. Rep.* **2016**, *6*, 29810. [CrossRef] [PubMed]
24. Lombrana, R.; Alvarez, A.; Fernandez-Justel, J.M.; Almeida, R.; Poza-Carrion, C.; Gomes, F.; Calzada, A.; Requena, J.M.; Gomez, M. Transcriptionally Driven DNA Replication Program of the Human Parasite *Leishmania major*. *Cell Rep.* **2016**, *16*, 1774–1786. [CrossRef] [PubMed]

25. Bottius, E.; Bakhsis, N.; Scherf, A. *Plasmodium falciparum* Telomerase: De Novo Telomere Addition to Telomeric and Nontelomeric Sequences and Role in Chromosome Healing. *Mol. Cell. Biol.* **1998**, *18*, 919–925. [CrossRef] [PubMed]
26. Raj, D.K.; Das, D.R.; Dash, A.P.; Supakar, P.C. Identification of telomerase activity in gametocytes of *Plasmodium falciparum*. *Biochem. Biophys. Res. Commun.* **2003**, *309*, 685–688. [CrossRef]
27. De Cian, A.; Grellier, P.; Mouray, E.; Depoix, D.; Bertrand, H.; Monchaud, D.; Telade-Fichou, M.-P.; Mergny, J.-L.; Alberti, P. *Plasmodium* Telomeric Sequences: Structure, Stability and Quadruplex Targeting by Small Compounds. *ChemBioChem* **2008**, *9*, 2730–2739. [CrossRef]
28. Kotha, S.; Mandal, K. Suzuki-Miyaura cross-coupling and ring-closing metathesis: A strategic combination for the synthesis of cyclophane derivatives. *Eur. J. Org. Chem.* **2006**, *23*, 5387–5393. [CrossRef]
29. Guillon, J.; Denevault-Sabourin, C.; Chevret, E.; Brachet-Botineau, M.; Milano, V.; Guédin-Beaurepaire, A.; Moreau, S.; Ronga, L.; Savrimoutou, S.; Rubio, S.; et al. Design, synthesis, and antiproliferative effect of 2,9-bis [4-(pyridinylalkylaminomethyl)phenyl]-1,10-phenanthroline derivatives on human leukemic cells by targeting G-quadruplex. *Arch. Pharm. (Weinheim)* **2021**, *354*, e2000450. [CrossRef]
30. Ramirez, T.; Strigun, A.; Verlohner, A.; Huener, H.A.; Peter, E.; Herold, M.; Bordag, N.; Mellert, W.; Walk, T.; Spitzer, M.; et al. Prediction of liver toxicity and mode of action using metabolomics in vitro in HepG2 cells. *Arch. Toxicol.* **2018**, *92*, 893–906. [CrossRef]
31. Rodriguez-Antona, C.; Donato, M.T.; Boobis, A.; Edwards, R.J.; Watts, P.S.; Castell, J.V.; Gómez-Lechón, M.J. Cytochrome P450 expression in human hepatocytes and hepatoma cell lines: Molecular mechanisms that determine lower expression in cultured cells. *Xenobiotica* **2002**, *32*, 505–520. [CrossRef]
32. Desjardins, R.E.; Canfield, C.J.; Haynes, J.D.; Chulay, J.D. Quantitative assessment of antimalarial activity *in vitro* by a semiautomated microdilution technique. *Antimicrob. Agents Chemother.* **1979**, *16*, 710–718. [CrossRef] [PubMed]
33. Bennett, T.N.; Paguio, M.; Gligorijevic, B.; Seudieu, C.; Kosar, A.D.; Davidson, E.; Roepe, P.D. Novel, Rapid, and Inexpensive Cell-Based Quantification of Antimalarial Drug Efficacy. *Antimicrob. Agents Chemother.* **2004**, *48*, 1807–1810. [CrossRef]
34. Bacon, D.J.; Latour, C.; Lucas, C.; Colina, O.; Ringwald, P.; Picot, S. Comparison of a SYBR Green I-Based Assay with a Histidine-Rich Protein II Enzyme-Linked Immunosorbent Assay for *In Vitro* Antimalarial Drug Efficacy Testing and Application to Clinical Isolates. *Antimicrob. Agents Chemother.* **2007**, *51*, 1172–1178. [CrossRef]
35. Kaddouri, H.; Nakache, S.; Houzé, S.; Mentré, F.; Le Bras, J. Assessment of the Drug Susceptibility of *Plasmodium falciparum* Clinical Isolates from Africa by Using a *Plasmodium* Lactate Dehydrogenase Immunodetection Assay and an Inhibitory Maximum Effect Model for Precise Measurement of the 50-Percent Inhibitory Concentration. *Antimicrob. Agents Chemother.* **2006**, *50*, 3343–3349.
36. Mosmann, T. Rapid colorimetric assay for cellular growth and survival: Application to proliferation and cytotoxicity assays. *J. Immunol. Methods* **1983**, *65*, 55–63. [CrossRef] [PubMed]
37. Emami, S.A.; Zamanai Taghizadeh Rabe, S.; Ahi, A.; Mahmoudi, M. Inhibitory Activity of Eleven *Artemisia* Species from Iran against *Leishmania* Major Parasites. *Iran J. Basic Med. Sci.* **2012**, *15*, 807–811. [PubMed]
38. De Cian, A.; Guittat, L.; Kaiser, M.; Saccà, B.; Amrane, S.; Bourdoncle, A.; Alberti, P.; Teulade-Fichou, M.-P.; Lacroix, L.; Mergny, J.-L. Fluorescence-based melting assays for studying quadruplex ligands. *Methods* **2007**, *42*, 183–195. [CrossRef] [PubMed]